Food and Chemical Toxicology 127 (2019) 237–250

Contents lists available at ScienceDirect

Food and Chemical Toxicology

journal homepage: www.elsevier.com/locate/foodchemtox

Multidirectional biological investigation and phytochemical profile of *Rubus sanctus* and *Rubus ibericus*

Gokhan Zengin[a,*], Claudio Ferrante[b], Ismail Senkardes[c], Reneta Gevrenova[d], Dimitrina Zheleva-Dimitrova[d], Luigi Menghini[b], Giustino Orlando[b,**], Lucia Recinella[b], Annalisa Chiavaroli[b], Sheila Leone[b], Luigi Brunetti[b], Carene Marie Nancy Picot-Allain[e], Kannan RR. Rengasamy[f], Mohamad Fawzi Mahomoodally[e]

[a] Department of Biology, Faculty of Science, Selcuk University, Konya, Turkey
[b] Department of Pharmacy, University "G. d'Annunzio" of Chieti-Pescara, Chieti, 66100, Italy
[c] Department of Pharmaceutical Botany, Faculty of Pharmacy, Marmara University, Istanbul, Turkey
[d] Department of Pharmacognosy, Faculty of Pharmacy, Medical University of Sofia, Bulgaria
[e] Department of Health Sciences, Faculty of Science, University of Mauritius, 230 Réduit, Mauritius
[f] Department of Bio-resources and Food Science, Konkuk University, Seoul, South Korea

ARTICLE INFO

Keywords:
Rubus
LC-MS
Toxicity
Antioxidant
Anti-inflammatory
Wound healing

ABSTRACT

In the present study, the biological properties, including, the enzyme inhibitory and antioxidant activities, as well as, the phytochemical profile of the ethyl acetate, methanol, and water extracts of *Rubus sanctus* Schreb. and *Rubus ibericus* Juz. leaves were determined using *in vitro* bioassays. Wide range of phytochemicals, including, hydroxybenzoic acids, hydroxycinnamic acids, acylquinic acids, ellagitannins, flavonoids, and triterpenoid saponins were determined using UHPLC-ESI/HRMS technique. The ethyl acetate and methanol extracts of the studied *Rubus* species effectively inhibited acetyl and butyryl cholinesterase. On the other hand, *R. sanctus* water extract showed low inhibition against α-amylase and prominent inhibitory action against α-glucosidase. Data collected from this study reported the radical scavenging and reducing potential of the studied *Rubus* species. Investigation of the protective effects of the different extracts of *R. sanctus* and *R. ibericus* in experimental model of ulcerative colitis was performed. The extracts were also tested on spontaneous migration of human colon cancer cells (HCT116) in wound healing experimental paradigm. Only *R. sanctus* methanol extract inhibited spontaneous HCT116 migration in the wound healing test. Our results suggested that *R. sanctus* and *R. ibericus* may be potential candidates as sources of biologically-active compounds for the development of nutraceuticals, pharmaceuticals, and/or cosmetics.

1. Introduction

The *Rubus* genus consists of 900–1000 species distributed worldwide (Ryu et al., 2018). Archaeologists found evidence of the use of *Rubus* dating around 8000 BCE, postulating that species of the *Rubus* genus have been long used as food and medicinal source (Hummer, 2010). Besides, ethnobotanical data substantiate the use of *Rubus* species for therapeutic applications by several cultures across the globe. For instance, the young shoots of the *Rubus* species were traditionally used to heal wounds, insect bites, and pimples (Süntar et al., 2011). The aerial part of *R. fruticosus* was used against cough, the fruit juice was recommended for colitis, the roots were used against diarrhoea, chewing the leaves of *R. fruticosus* was recommended to relieve toothache, a tea prepared from the roots was used for labour pain, and a decoction prepared from *R. fruticosus* roots was used to treat dysentery (Verma et al., 2014). Australian aborigines have long consumed *Rubus* fruits to induce mild laxative effect (Bakar et al., 2016). Indeed, *Rubus* fruits have long been consumed worldwide, for their possible health benefits or simply because of their good taste (Lee et al., 2012). A herbal tea prepared from the decoction of *R. sanctus* roots was used to alleviate pain and against rheumatism (Süntar et al., 2011). The fruits of *R. sanctus* were used as a diuretic and against diarrhoea, haemorrhoids, diabetes mellitus, and rheumatism (Akkol et al., 2015). *R. discolor* (synonym of *R. ibericus*) fruits, leaves, and roots were used to treat

* Corresponding author.
** Corresponding author.
E-mail addresses: gokhanzengin@selcuk.edu.tr (G. Zengin), giustino.orlando@unich.it (G. Orlando).

https://doi.org/10.1016/j.fct.2019.03.041
Received 23 January 2019; Received in revised form 19 March 2019; Accepted 20 March 2019
Available online 23 March 2019
0278-6915/

nephritis and prostatitis. Additionally, the leaves were used to heal wounds and treat diarrhoea (Veličković et al., 2016). In Traditional Chinese Medicine, a mixture containing *R. chingii* was used to manage infertility, impotence, frequent urination, low backache, and poor sight (Bakar et al., 2016). *R. parvifolius* roots were widely used for the treatment of hepatitis, rheumatism, and abdominal pain caused by postpartum stasis (Xu et al., 2017). Traditionally, teas and alcoholic infusions prepared from the leaves, shoots, and fruits of *R. grandifolius* were used for the management of diabetes, as depurative, diuretic, and to treat sore throat (Spínola et al., 2019).

Rubus species are rich sources of bioactive compounds, possessing multiple biological properties. Several studies reported the biological activities of *Rubus* species. For instance, euscaphic acid, isolated from *R. rosifolius*, has been reported to show significant antioxidant activity. Ellagic acid, quercetin, and kaempferol, identified from *R. rosifolius* were related to the chemopreventive properties of the plant (Campbell et al., 2017). Phenolic rich extracts of *R. rosifolius* presented antimicrobial properties with anti-quorum sensing properties and antioxidant activity (Oliveira et al., 2016). Three compounds isolated from *R. idaeus* rhizome showed neuroprotective effects *in vitro* (Xu et al., 2017). *R. hirsutus* fruits showed high antioxidant activity (Fu et al., 2015). *R. grandifolius* extracts inhibited α-glucosidase, β-glucosidase, α-amylase, lipase, and aldose reductase (Spínola et al., 2019). *R. fairholmianus* methanol root extract effectively lowered cell viability, ATP proliferation, and increased LDH release from human breast cancer cells (George et al., 2017). Previously, Shin et al. (2014) demonstrated protective effects induced by *R. coreanus* in experimental model of ulcerative colitis. Akkol et al. (2015) demonstrated the inhibitory action of extracts of *R. sanctus* aerial parts on collagenase and elastase.

Based on the multiple biological activities of several Rubus species, this study was designed to assess the possible inhibitory action of *R. sanctus* and *R. ibericus* against key enzymes relevant to Alzheimer's disease (acetyl and butyryl cholinesterases), skin hyperpigmentation complications (tyrosinase), and type 2 diabetes (α-amylase, and α-glucosidase). Besides, as far as our literature review could ascertain, there has not been any study on the inhibitory action of *R. sanctus* and *R. ibericus* on the selected enzymes. The antioxidant potential of the selected *Rubus* species was also evaluated. The phytochemical profiles of the ethyl acetate, methanol, and water extracts of *R. sanctus* and *R. ibericus* were determined by UHPLC-ESI/HRMS. The protective effects of *R. sanctus* and *R. ibericus* extracts, in an experimental model of ulcerative colitis constituted of rat colon specimens challenged with lipopolysaccharide (LPS) *ex vivo*, was assessed. Finally, the chemopreventive effects of *R. sanctus* and *R. ibericus* extracts on human colon cancer (HCT116) cell migration and invasion capacities (wound healing test) were investigated.

2. Materials and methods

2.1. Plant materials

The *Rubus* species were collected in Kastamonu-Turkey (*R. ibericus*: Hanönü village, between Yeniköy and Yılanlı, 619 m; *R. sanctus*: Hanönü village, centre of Yılanlı, 1015 m) in June 2018. The taxonomical identification was performed by the botanist Dr. Ismail Senkardes (Marmara University, Faculty of Pharmacy, Pharmaceutical Botany, Istanbul) and a voucher specimen of each species was kept in the herbarium of Marmara University. The leaves were allowed to dry for 10 days at the room temperature. Then, these samples were pulverised with a laboratory mill.

2.2. Extraction

To prepare ethyl acetate and methanol extracts, the leaves samples (5 g in 100 mL solvent) were stirred overnight (24 h) at room temperature and filtered. After filtration, the extracts were concentrated using a rotary evaporator under vacuum at 40 °C. Water extract was prepared by boiling 5 g of leaves samples in 100 mL water for 20 min. The mixture was then filtered and dried by using a lyophiliser. The extracts were stored at +4 °C until further analysis.

2.3. Quantification of phytochemicals

With reference to our previous studies (Uysal et al., 2017), the total amount of phenolics (TPC) (by standard Folin-Ciocalteu method) and flavonoids (TFC) (by aluminum chloride method) were determined. The final results were expressed as equivalents of standard compounds, i.e., gallic acid (mg GAE/g) and rutin (mg RE/g) for TPC and TFC, respectively.

2.4. Metabolite profiling by UHPLC-ESI/HRMS

The UHPLC-ESI/HRMS analyses were achieved on a Q Exactive Plus heated electrospray ionization (HESI-II) – high resolution mass spectrometer (HRMS) (ThermoFisher Scientific, Inc., Bremen, Germany) equipped with an ultra-high-performance liquid chromatography (UHPLC) system Dionex Ultimate 3000RSLC (ThermoFisher Scientific, Inc.) (Zengin et al., 2017). The analytical details were given in Supplemental material.

2.5. Determination of antioxidant and enzyme inhibitory effects

The enzyme inhibitory activity of *R. ibericus* and *R. sanctus* extracts were tested against α-amylase, α-glucosidase, acetyl cholinesterase (AChE), butyryl cholinesterase (BChE), and tyrosinase. The procedures of these assays were reported in our earlier work (Uysal et al., 2017). The enzyme inhibitory effects were expressed as equivalents of acarbose (for α-amylase and α-glucosidase), galantamine (for AChE and BChE), and kojic acid (for tyrosinase).

Antioxidant capacity of *R. ibericus* and *R. sanctus* extracts were spectrophotometrically determined using different methods including phosphomolybdenum, radical scavenging assays (DPPH and ABTS), reducing potentials (FRAP and CUPRAC), and ferrous ion chelating. The results were expressed as trolox (mg TE/g) and ethylenediaminetetraacetic acid equivalents (mg EDTAE/g). The procedures of assays were reported in our earlier work (Uysal et al., 2017).

The results of antioxidant and enzyme inhibitory assays were statistically with one-way ANOVA (by Tukey's test, $p < 0.05$). The statistical procedures were performed by SPPS v. 17.0. Multivariate analysis (Pearson Correlation, heat map and Sparse Partial Least Squares (sPLS-DA) analysis) were performed by using R software v. 3.5.1.

2.6. Biological assays

2.6.1. Artemia salina lethality bioassay

Artemia salina cysts were hatched in oxygenated artificial sea water (1 g cysts/L). After 24 h, brine shrimp larvae were gently transferred with a pipette in 6 well plate containing 2 mL of *Rubus* extracts at different concentrations (0.1–20 mg/mL) in artificial sea water. Ten larvae per well were incubated at 25–28 °C for 24 h. After 24 h the number of living napulii were counted under light microscope and compared to control untreated group. Results were expressed as percentage of mortality calculated as:

$$\frac{T - S}{T} \times 100,$$

where, T is the total number of incubated larvae and S is the number of survival napulii. Living nauplii were considered those exhibiting light activating movements during 10 s of observation. For each experimental condition two replicates per plate were performed and experimental triplicates were performed in separate plates.

2.6.2. In vitro studies

The HCT116 cell lines were cultured in DMEM (Euroclone) supplemented with 10% (v/v) heat-inactivated fetal bovine serum and 1.2% (v/v) penicillin G/streptomycin in 75 cm^2 tissue culture flask (n = 5 individual culture flasks for each condition). The cultured cells were maintained in humidified incubator with 5% CO_2 at 37 °C.

For cell differentiation, HCT116 cell suspensions at a density of 1×10^6 cells/mL were treated with various concentrations (10, 50, and 100 ng/mL) of phorbol myristate acetate (PMA, Fluka) for 24 h or 48 h (induction phase). Thereafter, the PMA-treated cells were washed twice with ice-cold pH 7.4 phosphate buffer solution (PBS) to remove PMA and non-adherent cells, whereas the adherent cells were further maintained for 48 h (recovery phase). Morphology of cells was examined under an inverted phase-contrast microscope.

To assess the basal cytotoxicity of *R. sanctus* and *R. ibericus* extracts, a viability test was performed on 96 micro well plates, using 3-(4,5-dimethylthiazol-2-yl)-2,5-diphenyltetrazolium bromide (MTT) test. Cells were incubated with extracts (ranging in the concentration 10–1000 μg/mL) for 24 h. Aliquot of 10 μL of MTT (5 mg/mL) was added to each well and incubated for 3 h. The formazan dye formed was extracted with DMSO and absorbance was recorded as previously described (Menghini et al., 2018). Effects on cell viability were evaluated in comparison to untreated control group.

Finally, HCT116 cell line was exposed to *Rubus* extracts, in wound healing experimental paradigm. HCT116 cells (6×10^3 cells/well) were seeded on 6-well plastic plates. Cells monolayers were preliminarily treated with a proliferation inhibitor mitomycin C (Sigma-Aldrich, St. Louis, Missouri, USA) at the non-toxic concentration of 5 μM, in order to exclude the effect of cell proliferation. After 2 h on cells in the confluence interval 85–90%, a wound was generated by scratching the cell monolayer using a 0–200 μL pipette tip. The sample was washed twice with PBS to remove detached cells. Cells were incubated in serum free media supplemented with Rubus extracts at the non-toxic concentration of 100 μg/mL. Cell migration was visualised by capturing at least 3 microscope images/well at time 0, 24 and 48 h. An inverted light microscope Leika equipped with Nikon 5100 camera was used to capture image at 4x magnification. The quantification of scratch area with no cells was quantified using Image-J software (NIH). Using GraphPad software (version 6.0), mean data at T0, 24 and 48 h were calculated for untreated control and *Rubus* extracts and expressed as percentage variation with reference to relative 100% of at 0 h.

2.6.3. Ex vivo studies

Male adult Sprague-Dawley rats (200–250 g) were housed in Plexiglass cages (40 cm × 25 cm × 15 cm), two rats per cage, in air-conditioned colony rooms (22 ± 1 °C; 60% humidity), on a 12 h/12 h light/dark cycle (light phase: 07:00–19:00 h), with free access to tap water and food, 24 h/day throughout the study, with no fasting periods. Rats were fed a standard laboratory diet (3.5% fat, 63% carbohydrate, 14% protein, 19.5% other components without caloric value; 3.20 kcal/g). Housing conditions and experimentation procedures were strictly in accordance with the European Union ethical regulations on the care of animals for scientific research.

The experiments were approved by Local Ethical Committee (University "G. d'Annunzio" of Chieti-Pescara) and Italian Health Ministry (Italian Health Ministry authorization N. F4738.N.XTQ, delivered on 11th November 2018). Rats were sacrificed by CO_2 inhalation (100% CO_2 at a flow rate of 20% of the chamber volume per min) and colon specimens were immediately collected and maintained in humidified incubator with 5% CO_2 at 37 °C for 4 h, in RPMI buffer with added bacterial LPS (10 μg/mL) (incubation period).

During the incubation period, tissues were treated with scalar subtoxic concentrations of *R. sanctus* and *R. ibericus* extracts (100 μg/mL). The activity of extracts was compared to sulfasalazine (2 mg/mL), an anti-inflammatory reference drug. Tissue supernatants were collected, and nitrite production was determined by mixing 50 μL of the assay buffer with 50 μL of Griess reagent (1.5% sulfanilamide in 1 M HCl plus 0.15% N-(1-naphthyl) ethylenediamine dihydrochloride in distilled water, [v/v]). After 10 min incubation at room temperature, the absorbance at 540 nm was determined and nitrite concentrations were calculated from a sodium nitrite standard curve.

On the other hand, individual colon specimens were dissected and subjected to extractive procedures to evaluate serotonin 5-hydroxytrptamine (5-HT) (ng/mg wet tissue) as previously reported (Brunetti et al., 2014; Ferrante et al., 2016). As regards to 5-HT analysis, tissues were homogenized in ice bath for 2 min with Potter-Elvehjem homogenizer in 1 mL of 0.05 N perchloric acid containing 0.004% sodium EDTA and 0.010% sodium bisulfite. Thereafter, samples were analyzed by HPLC coupled to electrochemical detection consisting of ESA Coulochem III detector equipped with ESA 5014B analytical cell.

Additionally, malondialdehyde (MDA) level was determined by the thiobarbituric acid reactive substances (TBARS) method (Mihara et al., 1980). Briefly, tissue specimens were added with 1% H_3PO_4 and 0.6% thiobarbituric acid, and then incubated at 96 °C for 20 min. Absorbance was recorded at 532 nm, and the MDA level was expressed as g/mL.

Besides, LDH activity was measured by evaluating the consumption of NADH in 20 mM HEPES-K^+ (pH 7.2), 0.05% bovine serum albumin, 20 μM NADH and 2 mM pyruvate using a microplate reader (excitation 340 nm, emission 460 nm) according to manufacturer's protocol (Sigma-Aldrich, St. Louis, Missouri, USA). Data were from triplicate test and expressed as relative variations compared to vehicle-treated cells (Menghini et al., 2018).

2.7. Statistical analysis

Statistical analysis was performed using GraphPad Prism version 5.01 for Windows (GraphPad Software, San Diego, CA). Means ± S.E.M. were determined for each experimental group and analyzed by one-way analysis of variance (ANOVA), followed by Newman-Keuls comparison multiple test. Statistical significance was considered as $p < 0.05$. Regarding the animals randomized for each experimental group, the number was calculated on the basis of the "Resource Equation" $N = (E + T)/T$ $(10 \leq E \leq 20)$ (Charan and Kantharia, 2013), and in accordance with the guidelines suggested by the "National Centre for the Replacement, Refinement and Reduction of Animals in Research" (NC3RS) and reported on the following web site: https://www.nc3rs.org.uk/experimental-designstatistics. N is the number of animals per treated group. E represents the degrees of freedom of the analysis of variance (ANOVA). T is the number of treatments. Considering that E values should be between 10 and 20, the animal number N for *ex vivo* analysis was chosen in accordance to an E value of 20.

3. Results and discussion

3.1. Quantification of total bioactive components

The Folin-Ciocalteu and aluminum chloride assays are rapid and simple quantitative phytochemical analyses currently used for the detection of bioactive secondary metabolites, namely, phenolics and flavonoids. Phenolics, consisting of one or more aromatic rings linked hydroxyl groups, are the most abundant class of secondary metabolites, involved in the reproductive, growth, and defence mechanisms of plants (Huot et al., 2014). The total phenolic content of the studied extracts ranged between 17.22 and 152.55 mg GAE/g extract and *R. ibericus* water extract showed the highest total phenolic content (Table 1). Likewise, Veličković et al. (2016) also reported that the aqueous extracts of *R. ibericus* leaves contained highest phenolic content. Flavonoids are a subclass of phenolic compounds and are well known for their antioxidant properties (Chen et al., 2018). In the present study, the total flavonoid content of the studied extracts ranged between 25.70 and 40.52 mg RE/g extract and *R. ibericus* ethyl acetate

Table 1
Total phenolic and flavonoid contents of *Rubus sanctus* and *R. ibericus* extracts.

Extract	Total phenolic content (mg GAE/g extract)	Total flavonoid content (mg RE/g extract)
R. sanctus-EA	17.22 ± 1.21^{e}	25.70 ± 0.62^{d}
R. sanctus -MeOH	83.31 ± 2.75^{d}	29.12 ± 0.59^{c}
R. sanctus -Water	134.53 ± 2.45^{b}	35.40 ± 3.99^{b}
R. ibericus-EA	21.57 ± 0.50^{e}	40.52 ± 0.50^{a}
R. ibericus -MeOH	115.53 ± 3.88^{c}	27.88 ± 0.20^{cd}
R. ibericus -Water	152.55 ± 1.45^{a}	38.08 ± 0.23^{ab}

Values expressed are means ± S.D. of three parallel measurements. GAE: Gallic acid equivalent; RE: Rutin equivalent; EA: Ethyl acetate; MeOH: Methanol. Different superscripts indicate differences among the extracts ($p < 0.05$).

extract showed the highest total flavonoid content. A group of authors studied the flavonoid content of *R. ibericus* leaves collected from different locations and extracted the plant materials using different solvents. Flavonoid yield was higher when acetone was used as extraction solvent, the sample collected from the different regions showed distinct difference in flavonoid content (Veličković et al., 2016).

3.2. UHPLC-ESI/HRMS results

Based on the accurate mass measurements, MS/MS fragmentation patterns, relative abundance of the precursor and fragment ions, elemental compositions, monoisotopic peak profiles, as well as comparison with reference standards and literature data, a variety of *Rubus* compounds were identified or tentatively elucidated. For the majority of assayed compounds, the mass accuracy of M-H]$^-$ in MS/MS analyses was within a level of 5 ppm.

3.2.1. Hydroxybenzoic acids and hydroxycinnamic acids, and their derivatives

The total ion chromatograms for the tested extracts were given in supplementary material (Fig. S1). Hydroxybenzoic acids **2**, **4** and **9**, and hydroxycinnamic acids **6**, **8** and **12** were identified on the basis of the retention times, accurate masses, fragmentation patterns and comparison with authentic standards (Table 2). Peaks **1** ([M-H]$^-$ at *m/z* 331.067) and **3** ([M-H]$^-$ at *m/z* 315.072) yielded abundant fragment ions at *m/z* 169.013 [gallic acid-H]$^-$ and 153.018 [protocatechuic acid-H]$^-$, respectively, indicating the loss of 162 Da. Thus **1** and **3** were identified as gallic acid-*O*-hexoside and protocatechuic acid *O*-hexoside, respectively. In the same way, **5** and **7** were tentatively identified as two isomers of caffeic acid-*O*-hexoside. MS/MS spectra of **10** ([M-H]$^-$ at *m/z* 503.155) and **11** ([M-H]$^-$ at *m/z* 504.123) were acquired (Table 2). The base peak at *m/z* 161.023 [caffeic acid-H−H_2O]$^-$ together with fragment ions at *m/z* 179.034 [caffeic acid-H]$^-$ and 135.044 [caffeic acid-H−CO_2]$^-$ allowed to identify caffeic acid derivatives. Fragmentation pattern of **10** displayed subsequent losses of hexose units at *m/z* 341.0902 [M-H-Hex]$^-$ and 323.079 [M-H-2Hex]$^-$, indicating caffeoyl-dihexoside. Prominent ions at *m/z* 282.070 [M-H-caffeoyl-60]$^-$ (**11**), 252.060 ([M-H-caffeoyl-90]$^-$ and 222.049 ([M-H-caffeoyl-120]$^-$ were consistent with cross ring cleavages of the hexose unit $^{0,4}X^-$, $^{0,3}X^-$ and $^{0,2}X^-$, respectively. Thus, **11** was ascribed to dicaffeoyl-hexoside.

3.2.2. Ellagitannins and ellagic acid derivatives

The abundant peak **17** at *m/z* 300.999 ([M-H]$^-$) matched the standard reference ellagic acid. Ellagic acid-*O*-pentoside (**15**) and ellagic acid-*O*-deohyhexoside (**16**) were identified based on the prominent ion at *m/z* 300.999 and matching MS/MS fingerprint as **17**, and data published by (Oszmiański et al., 2015). Concerning compound **14** ([M-H]$^-$ at *m/z* 934.073), the loss of a hexahydroxydiphenoyl (HHDP) moiety (301 Da) at *m/z* 633.073 and a base peak at *m/z* 300.999 [ellagic acid-H]$^-$, along with fragment ions at *m/z* 257.009 [ellagic acid-H−CO_2]$^-$, 245.009 [ellagic acid-H-2CO]$^-$, 229.014 [ellagic acid-H−CO−CO_2]$^-$ and 217.014 [ellagic acid-H-3CO]$^-$, highlighted the presence of galloyl-bis-HHDP-hexoside. This compound could be related to the ellagitannins casuarictin/potentillin, previously reported in *Rubus* species (Donno et al., 2013; Oszmiański et al., 2015). Peak **13** ([M-H]$^-$ at *m/z* 1401.597) afforded prominent ions at *m/z* 633.0735 and 300.999 corresponding to galloyl-HHDP-hexose and ellagic acid, respectively. This fragmentation pattern could be tentatively assigned to lambertianin C (Oszmiański et al., 2015).

3.2.3. Acylquinic acids

Eighteen acylquinic acids were identified in the majority of the tested *Rubus* extracts (Table 2). Herein, the hydroxycinnamic acids are mainly linked to quinic acid. The assignment of the different acylquinic acids was based on the hierarchical key developed by Clifford and colleagues (Clifford et al., 2003, 2005). Peaks **18**, **20** and **21** were identified as 3-*O*−, 5-*O*− and 4-*O*-caffeoylquinic acids ([M-H]$^-$ at *m/z* 353.088), respectively, according to the relative abundance of the characteristic fragment ions at *m/z* 191.055 [quinic acid-H]$^-$, 179.034 [caffeic acid-H]$^-$ and 173.045 [quinic acid-H−H_2O]$^-$ and 135.044 [caffeic acid-H−CO_2]$^-$ (Clifford et al., 2003, 2005). Based on comparison with authentic standards, compounds **18** and **20** were identified as neochlorogenic and chlorogenic acid, respectively. In the same manner, peaks **19**, **24** and **25** were ascribed to 3-*O*−, 4-*O*− and 5-*O*-*p*-coumaroylquinic acids ([M-H]$^-$ at *m/z* 337.093), while peaks **23**, **26** and **27** ([M-H]$^-$ at *m/z* 367.103) were assigned as 1-*O*−, 4-*O*− and 5-*O*-feruloylquinic acid (Table 2). Among the diacylquinic acids, peaks **28**, **29** and **30** were related to 3,4-*O*−, 3,5-*O* and 4,5-*O*-dicaffeoylquinic acids ([M-H]$^-$ at *m/z* 515.120); **28** and **30** yielded indicative fragment ions at 173.045 together with 353.088 ([M-H-caffeoyl]$^-$, while the presence of **29** was evidenced by the relative abundance of the ions at 191, 179 and 135 (Clifford et al., 2003; Clifford et al., 2005; Zheleva-Dimitrova et al., 2017). Compounds **31–34**, [M-H]$^-$ at *m/z* 529.136 related to caffeoyl-feruloylquinic acid (Clifford et al., 2003, 2005). Furthermore, **31** and **34** were discernible by the base peaks at *m/z* 193.050 [ferulic acid-H]$^-$ and 135.044 [caffeic acid-H−CO_2]$^-$, respectively. The formation of the abundant fragment ion at *m/z* 367.104 [M-H-caffeoyl]$^-$ (86.1%) (**31**) was favored for 3-feruloyl-5-caffeoylquinic acid, while 3-caffeoyl-5-feruloylquinic acid was witnessed by the abundant ions at 179.034 [caffeic acid-H]$^-$ (62.8%) (**34**) together with 161.023 [caffeic acid-H−H_2O]$^-$ (53.8%). Typical ions of 4-feruloyl-5-caffeoylquinic acid (**32**) fragmentation were observed at *m/z* 173.045 (base peak), 367.103 (64.4%) and 193.050 (17.9%). By comparison with 1,5-dicaffeoylquinic acid (Clifford et al., 2005, 2007), **33** was assigned to 1-caffeoyl-5-feruloylquinic acid, evidenced by the fragment ions at *m/z* 161.023 (base peak) and 367.103 (20.3%).

3.2.4. Flavonoids

Five flavonoid aglycones **53–57** were tentatively identified in the studied extracts (Table 2). Regarding **53**, typical neutral losses of the flavonoid aglycones were observed at *m/z* 245.082 [M-H−CO_2]$^-$, 205.051 [M-H-3CO]$^-$, 203.070 [M-H−C_3O_2−H_2O]$^-$. Fragment ions at *m/z* 163.038 ($^{1,4}B^-$), 137.023 ($^{1,3}A^-$) and 121.028 ($^{1,2}B^-$) were attributed to the Retro-Diels Alder (RDA) cleavages of the flavonoid skeleton (de Rijke et al., 2006). Consequently, **53** was identified as epicatechin. Indeed, the most important fragmentation pattern for **54** (luteolin) is the RDA cleavage which afforded ions at *m/z* 133.028 ($^{1,3}B^-$), 151.003 ($^{1,3}A^-$) and 107.012 ($^{0,4}A^-$). Fragments at *m/z* 241.050 [M-H−CO_2]$^-$ and 201.018 [M-H-3CO]$^-$ had low abundance (below 1%) which is consistent with the previous study (Zheleva-Dimitrova et al., 2018). Regarding **55** (quercetin), the precursor ion at 301.036 gave a series of neutral losses at *m/z* 273.041 [M-H−CO]$^-$, 255.030 [M-H-2CO]$^-$, 229.050 [M-H−CO−CO_2]$^-$. RDA cleavage generated $^{1,3}A^-$ at *m/z* 151.003, $^{0,2}A^-$ at *m/z* 163.003, $^{1,2}A^-$ at *m/z* 178.998, $^{1,2}B^-$ at *m/z* 121.0287 and $^{0,4}A^-$ at *m/z* 107.012 (Table 2). It is worth noting that **57** (isorhamnetin) yielded fragment ion at *m/z*

Table 2
Metabolites detected in the extracts from *Rubus ibericus* and *R. sanctus*.

Peak №	Accurate mass $[M-H]^-$ *m/z*	Molecular formula $[M-H]^-$	MS/MS data *m/z*	t_R [1(4)] min	Exact mass $[M-H]^-$ *m/z*	Delta ppm	Tentative assignment	Reference Standard (RS)/Reference
Hydroxybenzoic and hydroxycinnamic acids and derivatives								
1	331.0672	$C_{13}H_{15}O_{10}$	331.0672 (100), 169.0132 (53.31), 151.0023 (16.51), 125.0230 (20.67)	0.99	331.0659	0.303	Gallic acid-*O*-hexoside[a,b,c,d,e,f]	
2	169.0132	$C_7H_5O_5$	169.0132 (31.85), 125.0230 (100)	1.18	169.0131	−6.133	Gallic acid[a,b,c,d,e,f]	RS
3	315.0724	$C_{13}H_{15}O_9$	315.0727 (36.24), 153.0183 (100), 123.0439 (2.15), 109.0281 (44.28)	1.91	315.0710	0.935	Protocatechuic acid-*O*-hexoside[a,b,c,d,e,f]	
4	153.0182	$C_7H_5O_4$	153.0188 (11.57), 109.0281 (100), 123.0439 (85.33)	2.24	153.0182	−7.659	Protocatechuic acid[a,b,c,d,e,f]	RS
5	341.0881	$C_{15}H_{17}O_9$	341.0881 (21.0), 323.0789 (21.0), 281.0667 (100), 251.0561(55.1), 221.0452 (48.8), 179.0341 (95.6), 161.0234 (68.63), 135.0439 (68.9)	2.91	341.0867	0.813	Caffeic acid-*O*-hexoside[a,b,c,d,e,f]	Clifford et al. (2007)
6	163.0390	$C_9H_7O_3$	163.0390 (23.64), 135.0438 (9.15), 119.0489 (100)	3.10	163.0389	−6.731	*p*-Coumaric acid[a,b,c,d,e,f]	RS
7	341.0887	$C_{15}H_{17}O_9$	341.0887 (21.9), 281.0667 (3.0), 251.0560 (62.1), 221.0453 (50.4), 179.0341 (100), 161.0234 (65.9), 135.0439 (72.3)	3.26	341.0867	2.770	Caffeic acid-*O*-hexoside isomer[a,b,c,d,e,f]	Clifford et al. (2007)
8	179.0341	$C_9H_7O_4$	179.0341 (17.47), 135.0439 (100)	3.72	179.0338	−5.150	Caffeic acid[a,b,d,e]	RS
9	153.0182	$C_7H_5O_4$	153.0182 (65.10), 135.0074 (28.61), 122.0362 (1.56), 109.0281 (100)	4.03	153.0182	−7.463	Gentisic acid[a,b,c,d,e,f]	RS
10	503.1440	$C_{21}H_{27}O_{14}$	503.1548 (48.8), 341.0902 (3.6), 323.0787 (21.6), 179.0344 (34.3), 161.0234 (100), 135.0437 (39.4)	6.29	503.1406	6.701	Caffeoyldihexoside[d,e]	Oszmiański et al. (2015)
11	504.1273	$C_{24}H_{24}O_{12}$	504.1234 (96.7), 342.0916 (18.0), 282.0702 (29.2), 252.0595 (20.7), 222.0487 (10.8), 179.0342 (46.9), 161.0234 (100), 135.0439 (45.7)	6.29	504.1234	−6.677	Dicaffeoyl-hexoside[a,b]	
12	163.0391	$C_9H_7O_3$	163.0390 (21.22), 135.0438 (4.12), 119.0489 (100)	7.04	163.0389	−6.056	*m*-Coumaric acid[d,e]	RS
Ellagitannins and ellagic acid derivatives								
13	1401.5967	$C_{66}H_{97}O_{32}$	1401.5967 (72.0), 897.0446 (7.7), 633.0735 (12.2), 300.9989 (100), 229.0138 (8.6)	4.34	1401.5968	−0.117	Ellagitannins (Lambertianin C)[d]	Oszmiański et al. (2015)
14	934.0726	$C_{41}H_{26}O_{26}$	934.0726 (39.8), 663.0733 (6.6), 300.9989 (100), 257.0090 (3.9), 245.0092 (2.8), 229.0137 (6.1), 217.0136 (1.5)	4.55	934.0718	0.847	Galloyl-bis-hexahydroxyphenoyl-hexoside[a,b,c,d,e,f]	Donno et al. (2013)
15	433.0415	$C_{19}H_{13}O_{12}$	433.0415 (100), 300.9990 (82.7), 257.0091 (1.3), 229.0142 (1.9)	4.76	433.0412	0.510	Ellagic acid-pentoside[a,b,c,d,e,f]	Oszmiański et al. (2015)
16	447.0571	$C_{20}H_{15}O_{12}$	447.0571 (82.7), 300.994 (47.7), 299.9912 (100)	4.95	477.0569	0.382	Ellagic acid-deoxyhexoside[d]	Oszmiański et al. (2015)
17	300.9991	$C_{14}H_6O_8$	300.9991 (100), 257.0092 (0.4), 245.0091 (2.3), 229.0140 (3.2), 217.0131 (0.6), 145.0281 (3.4), 117.0317 (1.3)	5.10	300.9990	0.396	Ellagic acid[a,b,c,d,e,f]	RS
Acylquinic acids								
18	353.0880	$C_{16}H_{17}O_9$	353.0880 (46.2), 191.0553 (100), 179.0342 (67.3), 173.0447 (2.0), 161.0235 (4.6), 135.0439 (50.5), 93.0331 (2.0)	2.48	353.0867	0.580	Neochlorogenic (3-caffeoylquinic) acid[a,b,c,d,e,f]	RS
19	337.0932	$C_{16}H_{17}O_8$	337.0932 (7.7), 191.0552 (7.6), 173.0443 (4.1), 163.0390 (100), 119.0489 (28.0), 93.0329 (2.7)	3.12	337.0929	0.829	3-coumaroyl-quinic acid[a,b,c,d,e,f]	Clifford et al. (2005)
20	353.0881	$C_{16}H_{17}O_9$	353.0881 (6.0), 191.0554 (100), 179.0345 (3.1), 173.0450 (2.5), 161.0234 (2.3), 111.0433 (1.1), 97.4881 (0.7), 93.0331 (3.1), 127.0389 (1.7), 135.0439 (2.6)	3.29	353.0867	0.920	Chlorogenic (5-caffeoylquinic) acid[a,b,c,d,e,f]	RS
21	353.0881	$C_{16}H_{17}O_9$	353.0881 (28.3)191.0554 (56.1), 179.0341 (64.6), 173.0446 (100), 161.0229 (3.8), 135.0439 (58.8), 111.0438 (3.2), 93.0331 (21.8)	3.47	353.0867	0.920	4-caffeoylquinic acid[a,b,c,d,d,e,f]	Clifford et al. (2005)
22	367.1035	$C_{17}H_{19}O_9$	367.1035 (14.7), 193.0499 (100), 173.0448 (5.3), 149.0593 (2.4), 134.0361 (58.6), 93.0331 (2.6)	3.53	367.1035	0.094	3-feruloylquinic acid[a,b,c,d,e,f]	Clifford et al. (2005)
23	367.1038	$C_{17}H_{19}O_9$	367.1038 (41.0), 193.0499 (16.1), 173.0444 (2.6), 161.0233 (100), 134.0362 (9.1), 127.0388 (1.5), 85.0280 (12.4)	3.94	367.1035	0.830	1-feruloylquinic acid[a,d]	Clifford et al. (2005)
24	337.0929	$C_{16}H_{17}O_8$	337.0929 (7.3), 191.0555 (0.5), 173.0446 (100), 163.0390 (20.0), 119.0400 (7.3), 93.0331 (19.1), 97.4970 (0.7)	4.12	337.0929	0.473	4-coumaroyl-quinic acid[a,b,c,d,e,f]	Clifford et al. (2005)
25	337.0939	$C_{16}H_{17}O_8$	337.0939 (8.6), 191.0554 (100), 173.0444 (15.9), 163.0393 (6.4), 119.0489 (6.2), 93.0330 (20.1)	4.14	337.0929	4.532	5-coumaroyl-quinic acid[d,e]	Clifford et al. (2005)
26	367.1038	$C_{17}H_{19}O_9$	367.1038 (13.7), 193.0500 (18.0), 191.0552 (5.7), 173.0446 (100), 161.0230 (3.83), 134.0361 (14.8), 111.0439 (2.4), 93.0331 (24.2)	4.50	367.1034	−1.840	4-feruloylquinic acid[a,b,c,d,e,f]	Clifford et al. (2005)
27	367.1034	$C_{17}H_{19}O_9$	367.1034 (62.8), 193.0501 (0.7), 173.0445 (3.80), 161.0.234 (100), 134.0327 (1.0), 127.0388 (2.5), 111.0438 (0.4), 93.0332 (2.5), 85.0280 (17.0)	4.65	367.1034	−0.260	5-feruloylquinic acid[a,d]	Clifford et al. (2005)

(*continued on next page*)

Table 2 (*continued*)

Peak №	Accurate mass $[M-H]^-$ *m/z*	Molecular formula $[M-H]^-$	MS/MS data *m/z*	t_R[1(4)] min	Exact mass $[M-H]^-$ *m/z*	Delta ppm	Tentative assignment	Reference Standard (RS)/Reference
28	515.1198	$C_{25}H_{23}O_{12}$	515.1198 (100), 353.0883 (17.8), 335.0774 (8.2), 203.0335 (0.5), 191.0554 (41.55), 179.0341 (67.0), 173.0447 (78.8), 161.0234 (24.8), 135.0439 (67.8), 111.0436 (1.7), 93.0331 (19.8)	5.78	515.1184	0.487	3,4-dicaffeoylquinic acid[a,b,c,d,e,f]	Clifford et al. (2005)
29	515.1199	$C_{25}H_{23}O_{12}$	515.1199 (13.8), 353.0879 (93.8), 335.0776 (0.8), 191.0553 (100), 179.0341 (49.9), 173.0477 (4.66), 161.0284 (5.50), 135.0439 (50.3), 111.0438 (1.64), 93.0331 (3.7), 85.0279 (8.0)	5.94	515.1184	0.720	3,5-dicaffeoylquinic acid[a,b,c,d,e,f]	Clifford et al. (2005)
30	515.1196	$C_{25}H_{23}O_{12}$	515.1196 (6.3), 353.0880 (48.9), 335.0781 (1.1), 191.0554 (38.2), 179.0341 (68.5), 173.0446 (100), 161.0235 (6.0), 135.0439 (65.6), 11.0437 (1.2), 93.0331 (23.7), 85.0279 (6.2)	6.32	515.1184	0.254	4,5-dicaffeoylquinic acid[a,b,c,d,e,f]	Clifford et al. (2005)
31	529.1354	$C_{26}H_{25}O_{12}$	529.1354 (7.2), 367.1035 (86.1), 193.0500 (100), 161.0236 (77.7), 134.0361 (63.3),	6.92	529.1351	0.549	3-feruloyl-5- caffeoylquinic acid[a,b]	Clifford et al. (2005)
32	529.1350	$C_{26}H_{25}O_{12}$	529.1350 (74.0), 367.1030 (64.4), 193.0503(17.9), 173.0448(100), 134.0362 (14.8), 111.0439 (4.2), 93.0332 (24.5)	7.26	529.1351	−0.263	4-feruloyl-5- caffeoylquinic acid[a,b]	Clifford et al. (2005)
33	529.1357	$C_{26}H_{25}O_{12}$	529.1357 (7.2), 367.1032 (20.3), 349.0930 (2.8), 191.1402 (1.8), 161.0234 (100), 134.0355 (2.0), 93.0329 (1.7)	7.32	529.1351	1.003	1-caffeoyl-5-feruloylquinic acid[a,d]	Clifford et al. (2005)
34	529.1357	$C_{26}H_{25}O_{12}$	529.1357 (77.1), 367.1054 (18.6), 191.0249 (2.2), 179.0339 (62.8), 161.0233 (53.8), 134.0366 (7.1), 135.0439 (100)	7.69	529.1351	1.116	3-caffeoyl-5-feruloylquinic acid[a,d]	Clifford et al. (2005)
35	677.1513	$C_{34}H_{29}O_{15}$	677.1513 (97.6), 515.1188 (44.4), 353.0874 (52.6), 335.0780 (15.4), 229.5099 (4.0), 191.0552 (51.5), 179.0341 (75.6), 173.0447 (93.7), 161.0234 (28.5), 135.0440 (100), 111.0435 (5.0), 93.0330 (24.5)	7.86	677.1512	0.172	3,4,5-tricaffeoylquinic acid[a,b]	Clifford et al. (2007)
Flavonoids								
36	609.1476	$C_{27}H_{29}O_{16}$	609.1476 (2.5), 447.0934 (28.7), 285.0409 (65.8), 255.0296 (56.5)	3.89	609.1461	2.515	Luteolin-*O*-dihexoside[a,d]	Ferreres et al. (2007)
37	6091467	$C_{27}H_{29}O_{16}$	609.1467 (97.6), 429.0856 (1.0), 285.0400 (51.9), 284.0327 (100), 255.0302 (58.7), 227.0346 (34.2), 163.0029 (1.4), 151.0027 (2.0), 107.0122 (1.5)	4.87	609.1461	0.923	Kaempferol-*O*-dihexoside[a,c,d,e,f]	Ferreres et al. (2007)
38	609.1462	$C_{27}H_{29}O_{16}$	609.1462 (100), 301.0349 (49.5), 300.0276 (87.9), 271.0247 (51.8), 255.0296 (22.1), 243.0293 (12.6), 227.0347 (1.6), 163.0028 (1.7), 151.0026 (8.6), 107.0125 (1.9)	5.14	609.1461	0.118	Quercetin-3-*O*-rutinoside (rutin) [a,b,c,d,e,f]	RS
39	463.0885	$C_{21}H_{19}O_{12}$	463.0885 (100), 301.0349 (53.2), 300.0277 (98.2), 271.0249 (56.4), 255.0297 (21.5), 243.0298 (11.2), 227.0344 (4.4), 151.0025 (9.9), 135.0070 (0.7), 107.0119 (2.0)	5.27	–	0.585	Quercetin-3-*O*-galactoside (Hyperoside)[a,b,c,d,e,f]	RS
40	579.1359	$C_{26}H_{27}O_{15}$	579.1359 (84.6), 429.0829 (1.4), 327.0502 (0.3), 309.0408 (0.5), 285.0398 (42.9), 284.0327 (100), 255.0296 (61.3), 227.0346 (40.3), 229.0503 (4.0), 211.0398 (2.2), 178.9976 (2.0), 163.0024 (1.4), 151.0024 (2.6), 135.0073 (1.4), 107.0124 (2.5)	5.28	579.1355	0.547	Kaempferol-2″−*O*-pentosylhexoside[a,b,c,d,e,f]	Ferreres et al. (2007)
41	477.0669	$C_{21}H_{17}O_{13}$	477.0669 (54.6), 301.0356 (100), 271.0251 (1.0), 255.0300 (4.2), 243.0296 (0.9), 227.0341 (2.3), 211.0392 (2.6), 178.9978 (9.2), 163.0026 (4.3), 151.0023 (25.4), 135.0072 (0.3), 121.0281 (7.0), 107.0124 (9.9)	5.33	477.0675	−1.203	Quercetin-*O*-hexuronide[a,b,c,d,e,f]	Oszmiański et al. (2015)
42	463.0882	$C_{21}H_{19}O_{12}$	463.0882 (97.6), 301.0348 (42.3), 300.0277 (100), 271.0249 (54.0), 255.0298 (21.4), 243.0297 (13.5), 227.0344 (3.1), 151.0025 (7.2), 147.0078 (0.2), 135.0073 (1.2), 107.0123 (3.0)	5.39	463.0882	0.002	Quercetin-3-*O*-glucoside (isoquercitrin)[a,b,c,d,e,f]	RS
43	461.0728	$C_{21}H_{17}O_{12}$	461.0728 (48.8), 357.0616 (0.8), 327.0498 (1.4), 297.0393 (0.3), 285.0406 (100), 241.0504 (1.0), 229.0515 (0.3), 217.0507 (1.3), 151.0025 (5.4), 133.0282 (11.1), 107.0124 (3.0)	5.48	461.0725	0.501	Luteolin-*O*-hexuronide[d,e,f]	de Rijke et al. (2006)
44	433.0805	$C_{20}H_{17}O_{11}$	433.0805 (100), 301.0356 (58.7), 300.0272 (98.4), 271.0248 (56.5), 255.0301 (18.9), 243.0303 (13.0), 151.0027 (4.4)	5.60	433.0776		Quercetin-*O*-pentoside[a,b,c]	Oszmiański et al. (2015)
45	593.1511	$C_{27}H_{29}O_{15}$	593.1511 (91.5), 285.0403 (100), 255.0300 (53.6), 229.0504 (8.4), 227.0346 (37.5), 161.0226 (1.0), 151.0023 (3.3), 135.0072 (1.0), 107.0126 (3.1)	5.74	593.1512	0.415	Kaempferol-3-*O*-rutinoside[d,e,f]	RS
46	447.0564	$C_{20}H_{15}O_{12}$	447.0564 (95.2), 315.0150 (100), 299.9913 (89.9), 270.9887 (34.7), 255.0299 (2.5), 227.0356 (1.1)	5.87	477.0569	0.110	Isorhamnetin-*O*-pentoside[a,b,c,d,e,f]	de Rijke et al. (2006)

(*continued on next page*)

Table 2 (*continued*)

Peak №	Accurate mass [M-H]$^-$ *m/z*	Molecular formula [M-H]$^-$	MS/MS data *m/z*	$t_R^{1(4)}$ min	Exact mass [M-H]$^-$ *m/z*	Delta ppm	Tentative assignment	Reference Standard (RS)/Reference
47	477.1020	$C_{22}H_{21}O_{12}$	477.1020 (100), 315.0497 (19.4), 314.0434 (60.7), 300.0272 (11.6), 299.0197 (14.4), 271.0249 (37.5), 243.0297 (24.6), 179.0340 (35.3), 161.0233 (24.4), 151.0023 (5.8), 135.0440 (29.5)	5.89	477.1038	−3.897	Isorhamnetin-3-*O*-glucoside[a,b,c,d,e,f]	RS
48	461.0732	$C_{21}H_{17}O_{12}$	461.0732 (9.5), 285.0406 (100), 257.0457 (4.1), 229.0502 (10.2), 211.0398 (2.2), 201.0548 (1.1), 151.0022 (1.1), 163.0029 (1.4), 135.0073 (1.5), 131.0492 (0.3), 107.0123 (2.8)	5.95	461.0725	1.368	Kaempferol-*O*-hexuronide[a,b,c,d,e,f]	Oszmiański et al. (2015)
49	447.0938	$C_{21}H_{19}O_{11}$	447.0938 (100), 285.0327 (28.2), 284.0397 (75.1), 255.0298 (57.6), 227.0346 (58.9), 151.0025 (2.8), 135.0073 (0.57), 107.0124 (1.1)	5.96	447.0933	1.041	Kaempferol-3-*O*-glucoside[a,b,c,d,e,f]	RS
50	447.0875	$C_{21}H_{19}O_{11}$	447.0938 (100), 285.0405 (77.8), 271.0249 (14.6), 243.0304 (16.7), 227.0337 (4.1), 151.0026 (3.7), 133.0281 (9.4), 107.0121 (2.6)	6.39	447.0933	−12.894	Luteolin-7-*O*-glucoside[a,b,c,d,f]	RS
51	609.1250	$C_{30}H_{25}O_{14}$	609.1250 (100), 447.0944 (5.3), 285.0406 (84.3), 255.0299 (30.0), 229.0506 (7.4), 227.0349 (22.9), 211.0394 (1.4), 179.0340 (13.0), 161.0234 (30.3), 151.0024 (2.2), 135.0439 (18.7), 107.0123 (2.3)	7.07	609.1250	0.035	Kaempferol-*O*-caffeoylhexoside[a,b,d]	de Rijke et al. (2006)
52	593.1306	$C_{30}H_{25}O_{13}$	593.1306 (100), 447.0936 (3.1), 285.0403 (82.8), 257.0457 (2.9), 255.0300 (56.4), 239.0346 (1.6), 229.0502 (6.9), 227.0347 (39.4), 211.0395 (3.30), 151.0026 (3.7), 119.0489 (3.8), 117.0332 (3.8), 107.0120 (2.9)	7.77	593.1301	0.937	Kaempferol-3-*O*-*p*-coumaroyl-glucoside (tiliroside)[a,b,c,d,e,f]	RS
53	289.0720	$C_{15}H_{13}O_6$	289.0720 (100), 245.0822 (41.2), 205.0505 (15.7), 203.0702 (18.9), 163.0383 (2.0), 137.0230 (18.0), 121.0279 (8.5)	3.99	289.0718	0.687	Epicatechin	RS
54	285.0406	$C_{15}H_9O_6$	285.0406 (100), 241.0498 (0.78), 201.0180 (0.7), 151.0025 (6.5), 133.0282 (26.5), 107.0124 (4.8)	7.69	285.0405	0.452	Luteolin[a,b,c,d,e,f]	RS
55	301.0360	$C_{15}H_9O_7$	301.0360 (100), 273.0412 (3.9), 255.0297 (3.5), 229.0499 (1.8), 178.9978 (25.4), 163.0027 (0.7), 151.0025 (49.5), 11.60 (121.0281 (15.2), 107.0124 (14.5)	7.70	301.0354	2.007	Quercetin[a,b,c,d,f]	RS
56	285.0404	$C_{15}H_9O_6$	285.0404 (−0.320), 239.0354 (1.0), 229.0512 (1.4), 107.0122 (1.2)	8.97	285.0405		Kaempferol[a,b,c,d,e,f]	RS
57	315.0515		315.0515 (81.4), 300.0277 (100), 301.0305 (10.5), 255.0302 (2.4), 243.0299 (1.7), 227.0351 (3.0)	8.98	315.0510	1.632	Isorhamnetin[a,b,c,d,e,f]	RS
Triterpenoid saponins								
58	711.3967	$C_{36}H_{57}O_{11}$	711.3967 (99.0), 665.3905 (13.6), 503.3378 (100), 485.3265 (2.0)	7.26	711.3961	0.865	Ilexosapogenin A-hexoside[a,b,c,d,e,f]	Jung et al. (2001)
59	679.3703	$C_{36}H_{55}O_{12}$	679.3703 (100), 517.3170 (32.9), 499.3042 (0.4), 473.3264 (0.4), 455.3171 (6.7), 437.3052 (2.5), 393.3796 (0.4)(	8.26	679.3699	0.588	Barrinic acid-hexoside[a,b,c,d,e,f]	Jung et al. (2001)
60	709.3809	$C_{37}H_{57}O_{13}$	709.3809 (77.8), 663.3756 (12.1), 501.3226 (100), 483.3106 (1.3), 455.3175 (0.6), 439.3161 (0.4), 437.3079 (0.5), 421.3124 (3.4)	8.36	709.3805	0.557	Hydroxygypsogenic acid-hexoside[a,b,c,d,e,f]	Jung et al. (2001)
61	679.3704	$C_{36}H_{55}O_{12}$	679.3704 (100), 517.3185 (31.6), 455.3193 (3.3), 437.3068 (2.5)	8.39	679.3699	0.677	Barrinic acid-hexoside isomer[a,b,c,d,e,f]	
62	709.3809	$C_{37}H_{57}O_{13}$	709.3808 (67.7), 663.3767 (10.4), 501.3225 (100), 483.3120 (4.4)	8.59	709.3805	0.472	Hydroxygypsogenic acid-hexoside isomer[a,b,c,d,e,f]	
63	695.4022	$C_{37}H_{59}O_{12}$	695.4022 (91.9), 649.3929 (16.5), 487.3429 (100), 423.3273 (3.4)	9.10	695.4012	1.380	Arjunolic acid-hexoside[a,b,c,d,e,f]	Jung et al. (2001)
64	695.4012	$C_{37}H_{59}O_{12}$	695.4022 (76.3), 649.3929 (10.5), 487.3429 (100)	9.31	695.4012	1.380	Arjunolic acid-hexoside isomer[a,b,c,d,e,f]	
65	503.3361	$C_{30}H_{47}O_6$	503.3361 (100), 485.3277 (6.7), 473.3252 (1.1), 459.3103 (12.2), 457.3341 (3.3), 441.3391 (9.1), 439.3219 (1.2), 421.3129 (3.1), 407.2959 (0.9)	11.49	503.3378	−3.482	Ilexosapogenin A[c,f]	Jung et al. (2001)
66	517.3173	$C_{30}H_{45}O_7$	517.3173 (100), 499.3062 (2.6), 473.3303 (3.9), 455.3168 (11.0), 439.2848 (3.5), 421.2749 (0.6)	12.12	517.3171	0.354	Barrinic acid[c,f]	Jung et al. (2001)
67	487.3430	$C_{30}H_{47}O_5$	487.3430 (100), 469.2954 (0.6), 441.2969 (2.4), 423.2913 (0.5), 407.2961 (17.2), 405.2784 (1.9), 389.2856 (.5)	13.21	487.3430	0.251	Arjunolic acid[c,f]	Jung et al. (2001)
68	501.3220	$C_{30}H_{45}O_6$	501.3230 (100), 483.3107 (2.8), 471.3132 (0.5), 455.3171 (1.5), 437.3069 (1.2), 421.3119 (8.0), 419.2961 (1.9), 401.2869 (1.6), 393.3166 (0.6)	13.84	501.3222	1.731	Hydroxygypsogenic acid[c,f]	Jung et al. (2001)

[a] *Rubus sanctus*-MeOH.
[b] *R. sanctus*-Water.
[c] *R. sanctus*-EA).
[d] *R. ibericus*-MeOH.
[e] *R. ibericus*-Water.
[f] *R. ibericus*-EA. $t_R^{1(4)}$ retention times are referred to *Rubus sanctus* methanolic extract (^{1}), *R. ibericus* methanolic extract (^{4}) and *R. ibericus* ethylacetate extract (^{6}).

301.031 [M-H−CH_3]$^-$ together with radical aglycone [M-H−CH_3]$^{\bullet-}$ at *m/z* 300.028 (base peak) as has been seen previously (Cuyckens and Claeys, 2004). The identification of aforementioned flavonoid aglycones was confirmed by comparison with authentic standards.

Three isobaric flavonoids **36–38** shared the same [M-H]$^-$ at *m/z* 609.146 (exact mass). The MS/MS spectra of **36** and **37** showed losses of two hexose units yielding aglycone at *m/z* 285.041. Concerning **37**, RDA cleavage $^{0,2}A^-$ at *m/z* 163.003 and $^{1,3}A^-$ at *m/z* 151.003 suggested flavonol kaempferol, supported by abundant fragment ions at *m/z* 255. 030 (−CH_2O) (51.8%) and 227.035 (−CH_2O−CO) (34.2%). The aglycone of **36** was consistent with luteolin, witnessed by $^{1,3}B^-$ at 133. 028. Consequently, **36** and **37** were tentatively identified as luteolin-*O*− and kaempferol-*O*-dihexoside, respectively. Compounds **38**, **39**, **41**, **42** and **44** afforded the same abundant ion at *m/z* 301.035 (6) [quercetin-H]$^-$ supported by the radical aglycone at *m/z* 300.027 (8) as was seen previously for the quercetin-3-*O*-glycosides (Cuyckens and Claeys, 2004). Based on fragmentation pattern and comparison with authentic standards, **38**, **39** and **42** were identified as rutin, hyperoside and isoquercitrin, respectively, while **41** and **44** were assigned to quercetin-*O*-glucuronide and quercetin-*O*-pentoside, respectively.

The fragmentation fingerprints of **40**, **45**, **48**, **49**, **51** and **52** were associated with kaempferol derivatives, witnessed by the abundant fragment ion at *m/z* 285.040 supported by the ions at *m/z* 255, 227, 211, 179, 163, 151, 135 and 107 (**40**). The fragmentation of [M-H]$^-$ at *m/z* 579.136 (**40**) yielded low abundant ions at *m/z* 429.083 [M-H-132-H_2O]$^-$, 327.050 [M-H-132-120]$^-$ and 309.041 [M-H-120-132-H_2O]$^-$ indicating the presence of hexose and pentose moieties. The loss of 150 Da (132 + 120) suggested that latter could be linked to the hydroxyl group of the primary hexose. Moreover, the ion at *m/z* 309 indicated that the pentose unit is linked at position 2″, since the fragment 120 Da ($^{0,2}X_0^-$) implies 3″, 4″, 5″and 6" (Ferreres et al., 2007). The presence of the radical aglycone at *m/z* 284.033 (base peak) was in agreement with 3-*O*-glycosidic bond of the primary hexose (Cuyckens and Claeys, 2004). Thus, **40** was tentatively identified as kaempferol-2″−*O*-pentosyl-3-*O*-hexoside. The fragmentation pathway of **51** and **52** involved consequent losses of caffeoyl and *p*-coumaroyl residue, respectively, at *m/z* 447.094, and hexose at *m/z* 285.041.

The caffeoyl residue (**51**) was evidenced by the prominent ions at *m/z* 179, 161 and 135, as was seen in caffeoylquinic acids (Table 2). Accordingly, **51** was assigned to kaempfero-*O*-caffeoylhexoside. Based on comparison with authentic standard, **52** was identified as kaempferol-3-*O*-(6-*p*-coumaroyl)-glucoside (tiliroside), commonly found in *Rubus* sp. (Gevrenova et al., 2013; Han et al., 2012). In the same way, retention times, fragmentation patterns and monoisotopic profiles of **45**, **47**, **49** and **50** were in good agreement with those of the reference standards kaempferol-3-*O*-rutinoside, isorhamnetin-3-*O*-glucoside, kaempferol-3-*O*-glucoside and luteolin-7-*O*-glucoside.

3.2.5. Triterpenoid saponins

MS/MS spectra of three isobaric pairs **59/61**, **60/62** and **63/64** were acquired (Table 2). Concerning **59/61**, the loss of a hexose unit afforded a fragment ion at *m/z* 517.317 corresponding to the [sapogenin-H]$^-$ which was consistent with a molecular formula $C_{30}H_{45}O_7$ (0.558 ppm). Its fragmentation pathway involved losses of 18 Da (H_2O) and 44 Da (CO_2), together with the concomitant losses of (H_2O + CO_2) at *m/z* 455.317, (2H_2O + CO_2) at *m/z* 437.305 and (2H_2O + 2CO_2) at *m/z* 393.380, suggesting triterpenoid acid with at least two tertiary hydroxyl groups (Sandjo et al., 2017). This conclusion was consistent with barrinic acid-hexoside previously identified in the roots of *Rubus ctaraegifolia* (Jung et al., 2001). Formate adducts [M + HCO_2]$^-$ were observed at *m/z* 709.381 (**60/62**) and 695.402 (**63/64**). Their sapogenins were ascribed to the hydroxygypsogenin and arjunolic acid, respectively (Jung et al., 2001). In addition, ilexosapogenin A-hexoside was evidenced as main triterpenoid saponins in all studied extracts (Table 2) (Jung et al., 2001). Barrinic acid (**66**) was the dominant compound in both ethyl acetate extracts together with the abundant sapogenins ilexosapogenin A (**65**), arjunolic acid (**67**) and hydroxygypsogenic acid (**68**) (Table 2).

3.3. Antioxidant capacity

To determine the antioxidant properties of the different extracts of *R. sanctus* and *R. ibericus*, several antioxidant assays were employed. The total antioxidant capacity of the extracts, measured using the phosphomolybdenum assay, followed this order water > methanol > ethyl acetate extracts. It is worth mentioning that the total antioxidant capacity corresponded with total phenolic determinations. Indeed, several reports have demonstrated the relationship between phenolic content and antioxidant activity (Amzad Hossain and Shah, 2015; Encarnação et al., 2016). The anti-radical activity of the extracts was assessed using the DPPH and ABTS assays. In general, the methanol and water extracts of the studied *Rubus* species showed good anti-radical activities. Free radicals, being unstable and highly reactive, are capable of damaging biological molecules leading to cell damage and homeostatic disruption (Lobo et al., 2010). Multiple lines of evidence support the free radical scavenging properties of several species of the *Rubus* genus (Bhandary et al., 2012; Ding, 2011; Venskutonis et al., 2007). Upon evaluation of the reducing activity of the different extracts of *R. sanctus* and *R. ibericus*, the water extracts of both *Rubus* species showed highest reducing potential against FRAP and CUPRAC (Table 3). It is worth mentioning that *R. ibericus* showed higher activity compared to *R. sanctus*. This finding is in line with Veličković et al. (2016) who reported that higher reducing activity of *R. ibericus* aqueous leaves extract in the FRAP assay. Besides, rutin, previously identified from the aqueous extract of *R. ibericus* leaves (Keser et al., 2015) and known to possess potent reducing action (Apak et al., 2008) might be responsible for the observed activity. The chelating potential of the different extracts of the studied Rubus species was also investigated. According to data presented in Table 3, the water extracts (52.20 and 59.83 mg EDTAE/g extract, for *R. sanctus* and *R. ibericus*, respectively) of both Rubus species showed higher chelating activity.

3.4. Enzyme inhibitory properties

We investigated the inhibitory activities of the ethyl acetate, methanol, and water extracts of *R. sanctus* and *R. ibericus* against enzymes related to Alzheimer's disease, skin hyperpigmentation complications, and diabetes type 2. As shown in Table 4, the ethyl acetate and methanol extracts inhibited both acetyl and butyryl cholinesterase. The development of cholinesterase inhibitors is still the most popular clinical strategy targeted for the management of Alzheimer's disease. In fact, in the brain of Alzheimer's disease patients, the abnormal low level of acetylcholine has been related to pathological features of Alzheimer's disease, particularly cognitive decline (Li et al., 2018). *R. coreanus* ethanol extract showed inhibitory activity against acetylcholinesterase *in vitro* and exerted memory ameliorating effects *in vivo* (Kim et al., 2013).

The ability of the extracts to inhibit tyrosinase was also established. In general, the ethyl acetate (121.55 and 124.28 mg KAE/g extract, for *R. sanctus* and *R. ibericus*, respectively) and methanol (131.44 and 132.05 mg KAE/g extract, for *R. sanctus* and *R. ibericus*, respectively) extracts of the studied *Rubus* species showed potent inhibitory action against tyrosinase. Plant extracts showing inhibitory activity towards skin-regulating enzymes, such as tyrosinase, are considered as promising candidates for the development of dermatological treatments and cosmetics as skin-whitening agents (Papaioanou et al., 2018).

In the present study, we assessed the ability of *R. sanctus* and *R. ibericus* extracts to inhibit the activity of α-amylase and α-glucosidase. The inhibition of carbohydrate hydrolysing enzymes is considered as an interesting therapeutic strategy to control glycaemic level (Zengin et al., 2018). However, it is worth mentioning that the excessive inhibition of α-amylase has been associated to a number of gastrointestinal complications caused by undigested food (Uysal et al., 2019). Thus, developing hypoglycaemic agents showing mild or no α-amylase inhibition and potent α-glucosidase inhibitory action is considered as the ideal therapeutic approach to the management of diabetes type 2. In the present study, *R. sanctus* water extract showed low inhibition against α-amylase (0.12 mmol ACAE/g extract) and prominent inhibitory action against α-glucosidase (24.85 mmol ACAE/g extract). Data collected from this study support the traditional use of *R. sanctus* leaves for the treatment of diabetes type 2 (Süntar et al., 2011).

We performed further statistical analysis to understand any relationship between total bioactive components and biological activities. As presented in Fig. 1, we observed strong correlation between total phenolic and antioxidant properties. It might be suggested that phenolics in the tested extracts were responsible for the observed antioxidant activities. However, weak correlation was noted between phenolics and enzyme inhibitory effects. In this sense, non-phenolic inhibitors could be attributed to observed enzyme inhibitory effects. Apparently, the extracts were divided depending on species in sPLS-DA analysis. Also, VIP values are higher than 1 for total flavonoid content, phosphomolybdenum and metal chelating assays, which are main parameters to divide the extracts as well as species.

3.5. Biological assays

As a preliminary approach to evaluate potential toxicity, the ethyl acetate, methanol, and water of the selected *Rubus* species, (0.1–100 mg/mL) were tested on brine shrimp lethality assay. *Artemia salina* Leach is commonly used to investigate toxicological activities of plant extracts (Ohikhena et al., 2016). The evaluation of *Rubus* extract toxicity revealed LC_{50} values in the range 2.52–5.12 mg/mL.

Based on LC_{50} values recorded, a concentration of 500 μg/mL was chosen for subsequent assessment on human colon cancer-derived HCT116 cell using the MTT test. The tested extracts (10–500 μg/mL) confirmed a good biocompatibility, as revealed by the null effect on cell line viability in the range (10–100 μg/mL). On the other hand, at the highest tested concentration (500 μg/mL) cell viability decreased under the limit of biocompatibility (viability ≥ 70%).

Furthermore, the effect of *Rubus* extracts on spontaneous HCT116 cell migration, up to 48 h after scratching stimulus, was assessed. Results revealed that most of the extracts were ineffective in modulating spontaneous HCT116 cell migration. By contrast, *R. sanctus* methanol extract significantly inhibited spontaneous cell migration thus suggesting a potential protective effect against migration and invasion capacities of HCT116 human colon cancer cells (Fig. 2).

A subsequent panel of experiments was performed on isolated rat colon specimens challenged with LPS, a validated *ex vivo* experimental paradigm to evaluate the efficacy of drugs and extracts on oxidative and inflammatory pathways involved in ulcerative colitis (Locatelli et al., 2017; Menghini et al., 2016, 2018). Overproduction of reactive oxygen/nitrogen species (ROS/RNS) has long been considered to play a key in tissue damage through disruptive peroxidation reactions on macromolecules, including proteins, lipids, and nucleic acids (Uttara et al., 2009). Particularly, lipid peroxidation has been long involved in tissue chronic inflammatory diseases (Achitei et al., 2013). The role of ROS/RNS, mainly synthesized by activated macrophages and neutrophils, include neutrophils recruitment at the inflamed tissues (Fialkow et al., 2007; Kruidenier and Verspaget, 2002). To this regard, the assessment of tissue nitrite level is a useful marker of nitric oxide (NO) synthesis, which is an indicator of disease activity in ulcerative colitis (Goggins et al., 2001). NO is a free radical which can react with

Table 3
Antioxidant activities of *Rubus sanctus* and *R. ibericus* extracts.

Extract	DPPH (mg TE/g extract)	ABTS (mg TE/g extract)	CUPRAC (mg TE/g extract)	FRAP (mg TE/g extract)	Phosphomolybdenum (mmol TE/g)	Metal chelating ability (mg EDTAE/g)
R. sanctus-EA	24.12 ± 0.81^{f}	28.19 ± 2.64^{e}	71.08 ± 6.40^{f}	26.81 ± 2.33^{e}	1.65 ± 0.03^{f}	46.91 ± 2.46^{c}
R. sanctus -MeOH	347.61 ± 13.21^{d}	279.95 ± 11.13^{d}	456.23 ± 5.56^{d}	245.93 ± 5.44^{d}	2.50 ± 0.12^{d}	39.68 ± 2.46^{d}
R. sanctus -Water	386.39 ± 10.97^{c}	543.68 ± 14.28^{b}	762.96 ± 2.95^{b}	486.85 ± 3.24^{b}	3.05 ± 0.04^{c}	52.20 ± 0.19^{b}
R. ibericus-EA	37.37 ± 0.66^{e}	34.15 ± 4.53^{e}	91.42 ± 1.45^{e}	32.89 ± 2.41^{e}	1.97 ± 0.04^{e}	47.30 ± 1.32^{c}
R. ibericus -MeOH	487.60 ± 0.93^{a}	483.51 ± 7.25^{c}	681.88 ± 5.44^{c}	416.13 ± 14.69^{c}	3.92 ± 0.10^{b}	53.27 ± 0.14^{b}
R. ibericus -Water	453.74 ± 11.99^{b}	663.40 ± 12.58^{a}	921.92 ± 6.85^{a}	616.63 ± 7.12^{a}	4.52 ± 0.06^{a}	59.83 ± 0.52^{a}

Values expressed are means ± S.D. of three parallel measurements. TE: Trolox equivalent; EDTAE: EDTA equivalent; EA: Ethyl acetate; MeOH: Methanol. Different superscripts indicate differences among the extracts ($p < 0.05$).

Table 4
Enzyme inhibitory properties of *Rubus sanctus* and *R. ibericus* extracts.

Extract	AChE (mg GALAE/g extract)	BChE (mg GALAE/g extract)	Tyrosinase (mg KAE/g extract)	α-amylase (mmol ACAE/g extract)	α-glucosidase (mmol ACAE/g extract)
R. sanctus-EA	2.88 ± 0.10^{b}	2.18 ± 0.31^{b}	121.55 ± 2.39^{b}	0.73 ± 0.05^{b}	23.30 ± 1.26^{b}
R. sanctus -MeOH	3.30 ± 0.21^{a}	1.41 ± 0.03^{c}	131.44 ± 0.37^{a}	0.72 ± 0.01^{b}	na
R. sanctus -Water	na	na	78.14 ± 3.23^{d}	0.12 ± 0.01^{c}	24.85 ± 0.53^{a}
R. ibericus-EA	2.28 ± 0.04^{c}	2.49 ± 0.24^{a}	124.28 ± 1.04^{b}	0.82 ± 0.06^{a}	24.67 ± 0.04^{a}
R. ibericus -MeOH	3.20 ± 0.05^{a}	0.27 ± 0.04^{d}	132.05 ± 1.57^{a}	0.67 ± 0.04^{b}	na
R. ibericus -Water	0.25 ± 0.06^{d}	na	83.99 ± 2.62^{c}	0.11 ± 0.01^{c}	na

Values expressed are means ± S.D. of three parallel measurements. GALAE: Galatamine equivalent; KAE: Kojic acid equivalent; ACAE: Acarbose equivalent; na: not active; EA: Ethyl acetate; MeOH: Methanol. Different superscripts indicate differences among the extracts ($p < 0.05$).

multiple tissue biomolecules, thus giving oxidation products including nitrite, nitrate, nitrosyl (NO-heme) species, and S− and N-nitroso products. The level of these NO-related products reflects the nitrosative stress due to inflammation-induced upregulation of the inducible NO synthase (iNOS) (Saijo et al., 2010).

R. sanctus methanol and ethyl acetate extracts were equally able to reduce LPS-induced nitrite level in isolated colon (Fig. 3), while sulfasalazine resulted ineffective in downregulating nitrite levels. The null effect of sulfasalazine on nitrite level corroborates with the recent findings by Cetin et al. (2017) which observed a null effect displayed by sulfasalazine on nitrosative stress pathway, evaluated as nitrite level. *R. sanctus* methanol and *R. ibericus* ethyl acetate extracts were also able to reduce colon MDA levels, upregulated by LPS challenging (Fig. 4). The extracts were as effective as sulfasalazine, which was able to restore basal MDA level in isolated rat colon challenged with LPS, according to the recent findings by Soliman et al. (2019). Consistent with the effect on MDA level, the extracts reduced LDH level on rat colon, showing activity as effective as sulfasalazine (Fig. 5). LDH could be considered a predictive marker of tissue damage, especially in the gut, and reduced LDH activity following extracts treatment was related to protective effects in IBDs (Kannan and Guruvayoorappan, 2013; Nagarjun et al., 2017). Actually, the downregulation of nitrite, MDA and LDH level induced by the extracts is consistent with their total phenol and flavonoid content (Raihan et al., 2009). The relative abundance in kaempferol could explain, albeit partially, the major blunting effect exerted by *R. sanctus* methanol extract on LPS-induced nitrite, MDA and LDH level, in isolated rat colon..

5-HT pro-inflammatory role in ulcerative colitis has been previously suggested (Regmi et al., 2014), possibly involving the activation of 5-HT3 receptors (Mousavizadeh et al., 2009). Previously, it was observed that antioxidant and anti-inflammatory chamomile and devil's claw extracts reduced 5-HT steady state level, in rat colon challenged with

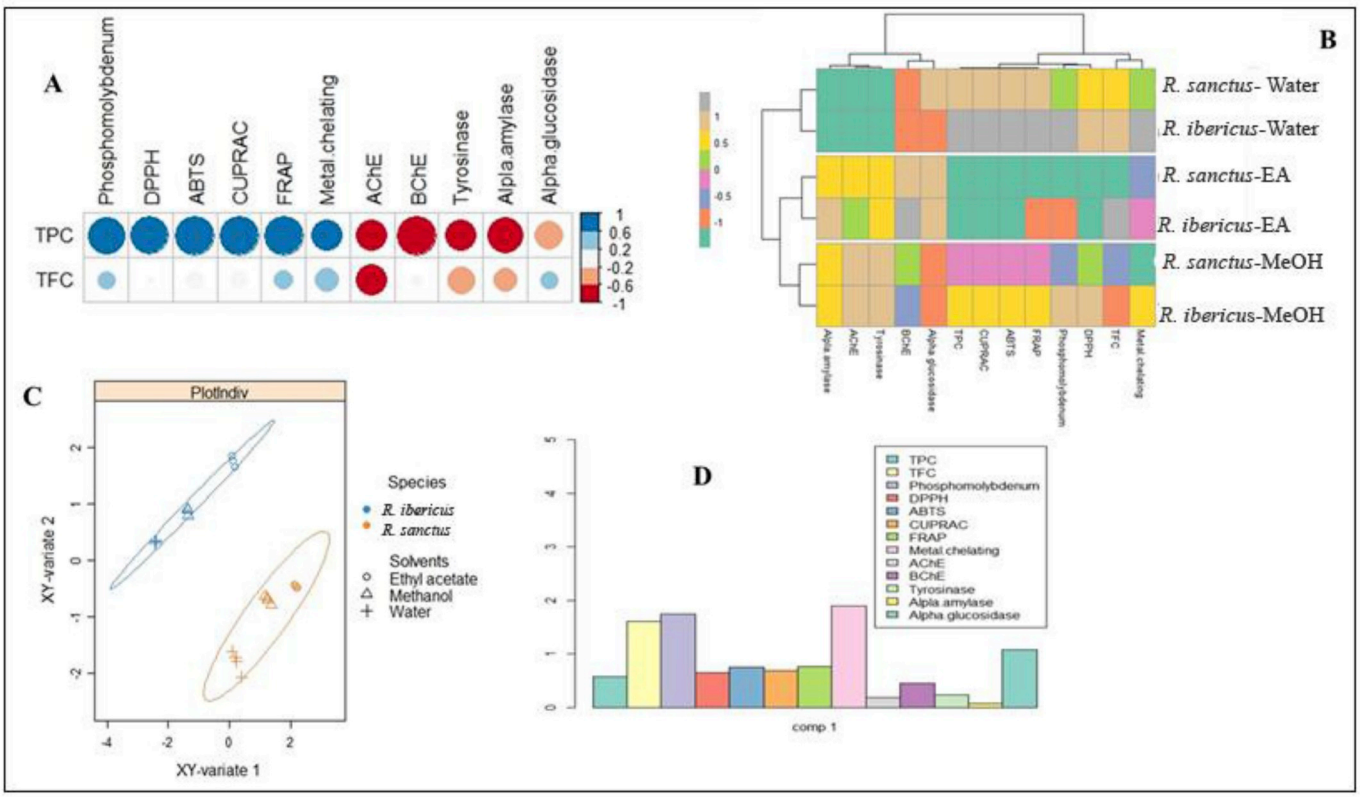

Fig. 1. Statistical Evaluation (**A:** Relationship between total bioactive compounds and biological activities; **B:** Clustering of extracts in according to biological activities and total bioactive components based on Heatmap; **C:** sPLS-DA results obtained from biologicals activities of the tested extracts; **D:** Influence of 13 variables (total bioactive components and biologicals activities) for the total map (VIP variable importance in the prediction).

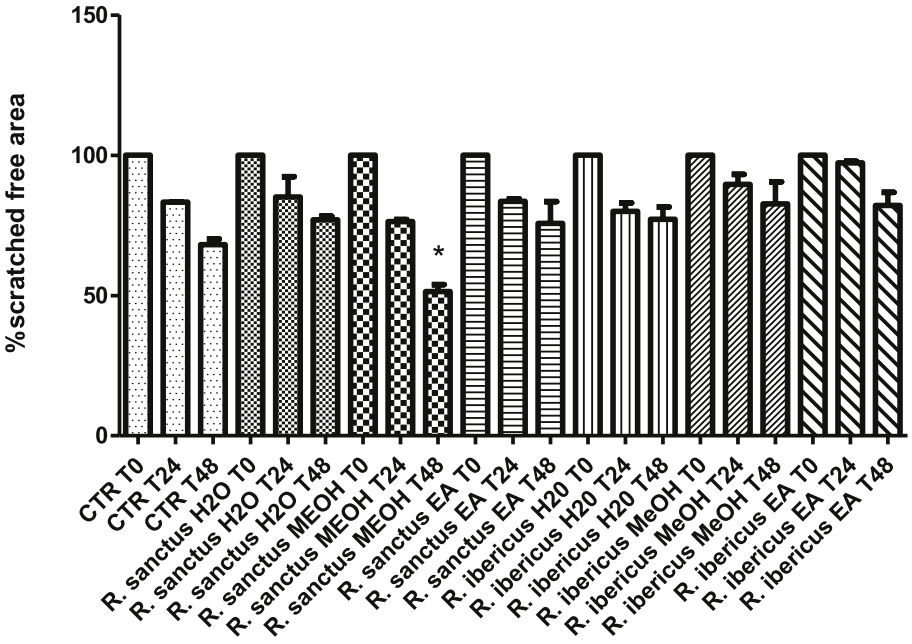

Fig. 2. Effect of MeOH, water and EA extracts (100 μg/mL) of *R. ibericus* and *R. sanctus* on spontaneous HCT116 cell migration (wound healing test). Data are means ± SD of three experiments performed in triplicate. ANOVA, $P < 0.05$; post-hoc, *$P < 0.05$ vs. CTR48.

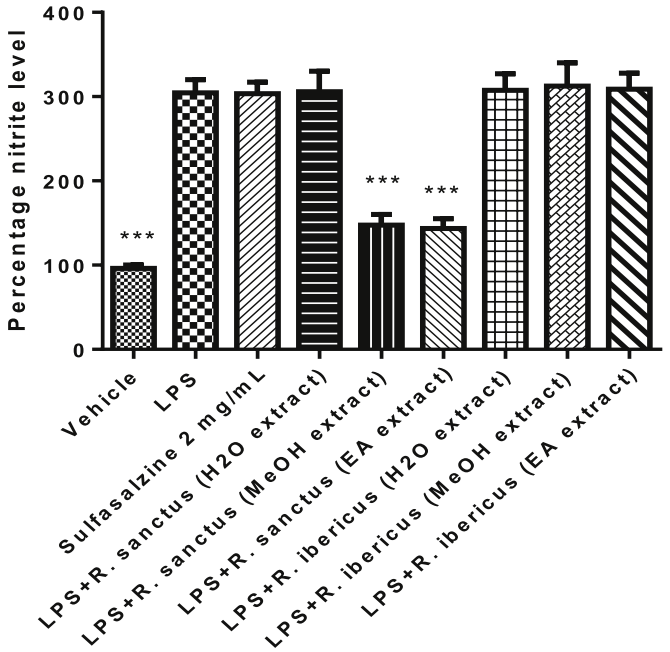

Fig. 3. Effect of MeOH, water and EA extracts (100 μg/mL) of *R. ibericus* and *R. sanctus* on LPS-induced nitrite level (mmoL/g wet tissue) in rat colon specimens (N = 5 per group). ANOVA, $P < 0.0001$; post-hoc, ***$P < 0.001$ vs. LPS.

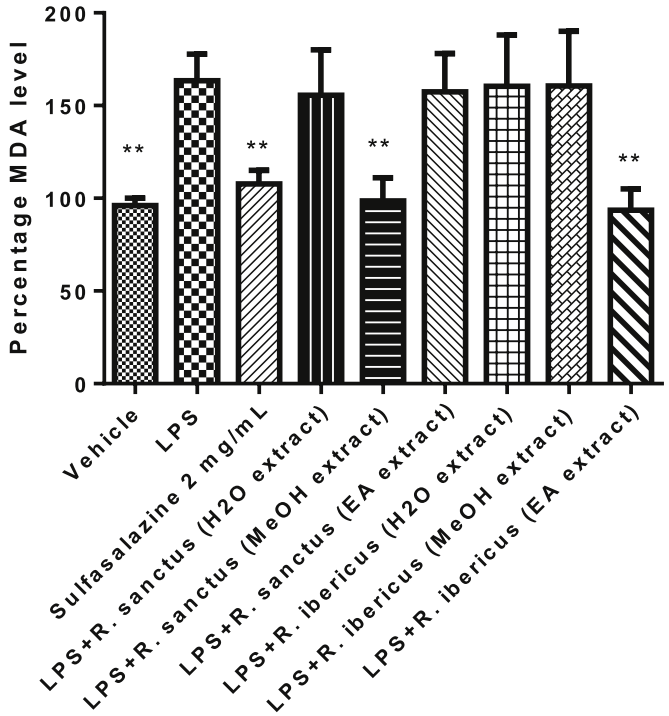

Fig. 4. Effect of MeOH, water and EA extracts (100 μg/mL) of *R. ibericus* and *R. sanctus* on LPS-induced malondialdehyde (MDA) production in rat colon tissues challenged with LPS (N = 5 per group). ANOVA, $P < 0.001$; post-hoc, **$P < 0.01$ vs. LPS.

LPS (Menghini et al., 2016). Several studies confirmed that steady state tissue 5-HT concentration also proved to be a valuable index of neurotransmitter activity, including synthesis and release (Bungo et al., 2009; Clark et al., 2006). Aqueous extracts from each species revealed equally effective in blunting LPS-induced 5-HT steady state levels, in rat colon (Fig. 6). Additionally, *R. sanctus* ethyl acetate extract revealed to be more effective than sulfasalazine (Menghini et al., 2016). The inhibitory effects exerted by *R. sanctus* and *R. ibericus* extracts could be related to multiple concomitant mechanisms. On one side, the phenol and flavonoid content could reduce 5-HT level as a result of the antioxidant activity. On the other side, the inhibitory effect on 5-HT activity could be induced by multiple components of flavonoid fraction which could reduce 5-HT release and antagonize pro-inflammatory 5-HT3

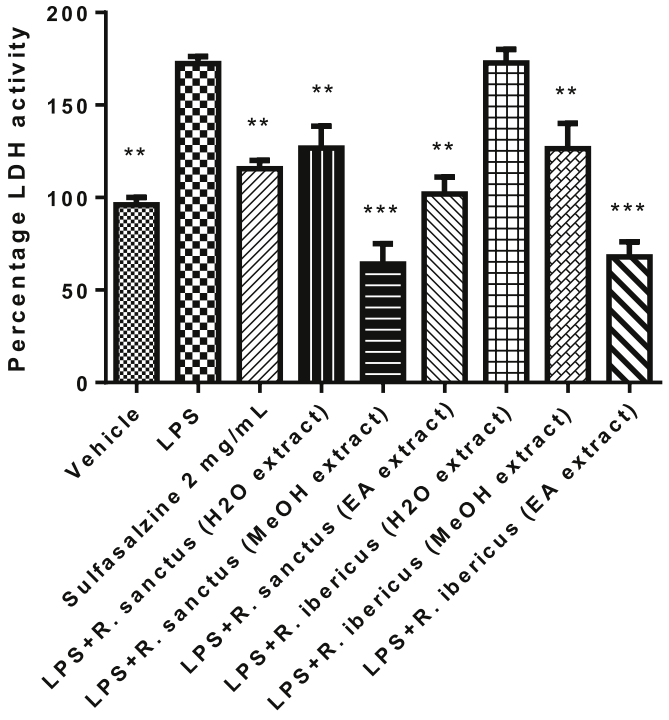

Fig. 5. Effect of MeOH, water and EA extracts (100 μg/mL) of *R. ibericus* and *R. sanctus* on LPS-induced lactate dehydrogenase (LDH) activity in rat colon specimens (N = 5 per group). ANOVA, P < 0.001; post-hoc, **P < 0.01, ***P < 0.001 vs. LPS.

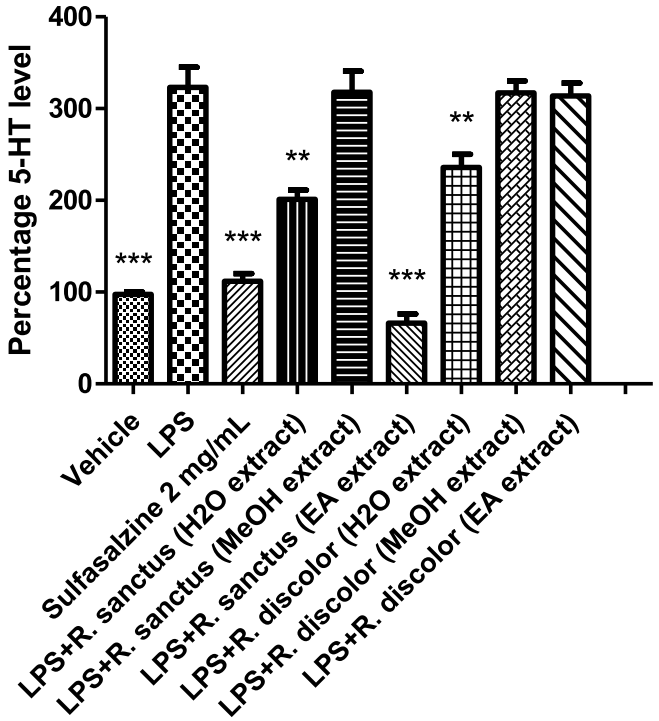

Fig. 6. Effect of MeOH, water and EA extracts (100 μg/mL) of *R. ibericus* and *R. sanctus* on serotonin (5-HT) level (ng/mg wet tissue) in rat colon specimens challenged with LPS (N = 5 per group). ANOVA, P < 0.001; post-hoc, **P < 0.01, ***P < 0.001 vs. LPS.

mediated-pathway. (Chen et al., 2002; Herbrechter et al., 2015).

4. Conclusion

Results of the present investigation revealed the potential of the selected *Rubus* species as effective enzyme inhibitors and antioxidant agents. Besides, findings of this study highlight the importance of solvent choice in the extraction of bioactive compounds from plants. The water extracts showed high phenolic content and antioxidant activity while the ethyl acetate and methanol extracts of *R. sanctus* and *R. ibericus* showed potent enzyme inhibitory activity. In the quest for safer hypoglycaemic agents, *R. sanctus* water extract revealed to be a promising candidate, showing low α-amylase inhibition and prominent α-glucosidase inhibitory activity.

On the other hand, *R. sanctus* methanol extract showed anti-inflammatory activity in colon cells, showing significant blunting effects on LPS-induced levels of well-established markers of oxidative stress and tissue damage such as nitrites, MDA, and LDH. Besides, *R. sanctus* methanol extract displayed a significant inhibition of spontaneous migration of HCT116 cell line, thus suggesting a potential protective effect against migration and invasion capacities of human colon cancer cells. Further studies are warranted to isolate and characterize bioactive compounds present in the studied *Rubus* extracts for the development of novel nutraceuticals, pharmaceuticals and/or cosmetics.

Conflicts of interest

The authors declare that there are no conflicts of interest.

Acknowledgements

The study was supported by Italian Ministry of University (FAR grants): FAR 2018 granted to Prof. Claudio Ferrante; FAR 2017 granted to Prof. Giustino Orlando.

Appendix A. Supplementary data

Supplementary data to this article can be found online at https://doi.org/10.1016/j.fct.2019.03.041.

References

Achitei, D., Ciobica, A., Balan, G., Gologan, E., Stanciu, C., Stefanescu, G., 2013. Different profile of peripheral antioxidant enzymes and lipid peroxidation in active and non-active inflammatory bowel disease patients. Dig. Dis. Sci. 58, 1244–1249.

Akkol, E.K., Süntar, I., Ilhan, M., Aras, E., 2015. In vitro enzyme inhibitory effects of *Rubus sanctus* Schreber and its active metabolite as a function of wound healing activity. J. Herb. Med. 5, 207–210.

Amzad Hossain, M., Shah, M.D., 2015. A study on the total phenols content and antioxidant activity of essential oil and different solvent extracts of endemic plant *Merremia borneensis*. Arab. J. Chem. 8, 66–71.

Apak, R., Güclü, K., Özyürek, M., Celik, S.E., 2008. Mechanism of antioxidant capacity assays and the CUPRAC (cupric ion reducing antioxidant capacity) assay. Microchim. Acta 160, 413–419.

Bakar, A., Fadzelly, M., Ismail, N.A., Isha, A., Ling, M., Lee, A., 2016. Phytochemical composition and biological activities of selected wild berries (*Rubus moluccanus* L., *R. fraxinifolius* Poir., and *R. alpestris* Blume). J. Evid. Based Complementary Altern. Med. 2016, 1–10.

Bhandary, B., Lee, H.Y., Back, H.I., Park, S.H., Kim, M.G., Kwon, J.W., Song, J.Y., Lee, H.K., Kim, H.R., Chae, S.W., Chae, H.J., 2012. Immature *Rubus coreanus* shows a free radical-scavenging effect and inhibits cholesterol synthesis and secretion in liver cells. Ind. J. Pharm. Sci. 74, 211–216.

Brunetti, L., Leone, S., Orlando, G., Ferrante, C., Recinella, L., Chiavaroli, A., Di Nisio, C.,

Shohreh, R., Manippa, F., Ricciuti, A., 2014. Hypotensive effects of omentin-1 related to increased adiponectin and decreased interleukin-6 in intra-thoracic pericardial adipose tissue. Pharmacol. Rep. 66, 991–995.
Bungo, T., Shiraishi, J.-i., Yanagita, K., Ohta, Y., Fujita, M., 2009. Effect of nociceptin/orphanin FQ on feeding behavior and hypothalamic neuropeptide expression in layer-type chicks. Gen. Comp. Endocrinol. 163, 47–51.
Campbell, T.F., McKenzie, J., Murray, J., Delgoda, R., Bowen-Forbes, C.S., 2017. *Rubus rosifolius* varieties as antioxidant and potential chemopreventive agents. J. Funct. Food. 37, 49–57.
Cetin, C., Erdogan, A.M., Dincel, G.C., Bakar, B., Kisa, U., 2017. Effects of sulphasalazine in cerebral ischemia reperfusion injury in rat. Arch. Med. Res. 48, 247–256.
Charan, J., Kantharia, N., 2013. How to calculate sample size in animal studies? J. Pharmacol. Pharmacother. 4, 303.
Chen, W., Jin, M., Wu, W., 2002. Experimental study on inhibitory effect of rutin against platelet activation induced by platelet activating factor in rabbits. Chin. J. Integr. Med. 22, 283–285.
Chen, X., Deng, Z., Zhang, C., Zheng, S., Pan, Y., Wang, H., Li, H., 2018. Is antioxidant activity of flavonoids mainly through the hydrogen-atom transfer mechanism? Food Res. Int. https://doi.org/10.1016/j.foodres.2018.11.018.
Clark, K.A., MohanKumar, S.M., Kasturi, B.S., MohanKumar, P., 2006. Effects of central and systemic administration of leptin on neurotransmitter concentrations in specific areas of the hypothalamus. Am. J. Physiol. Regul. Integr. 290, 306–312.
Clifford, M.N., Johnston, K.L., Knight, S., Kuhnert, N., 2003. Hierarchical scheme for LC-MSn identification of chlorogenic acids. J. Agric. Food Chem. 51, 2900–2911.
Clifford, M.N., Knight, S., Kuhnert, N., 2005. Discriminating between the six isomers of dicaffeoylquinic acid by LC-MSn. J. Agric. Food Chem. 53, 3821–3832.
Clifford, M.N., Wu, W., Kirkpatrick, J., Kuhnert, N., 2007. Profiling the chlorogenic acids and other caffeic acid derivatives of herbal Chrysanthemum by LC− MSn. J. Agric. Food Chem. 55, 929–936.
Cuyckens, F., Claeys, M., 2004. Mass spectrometry in the structural analysis of flavonoids. J. Mass Spectrom. 39, 1–15.
de Rijke, E., Out, P., Niessen, W.M., Ariese, F., Gooijer, C., Brinkman, U.A.T., 2006. Analytical separation and detection methods for flavonoids. J. Chromatogr. A 1112, 31–63.
Ding, H.Y., 2011. Extracts and constituents of *Rubus chingii* with 1,1-diphenyl-2-picrylhydrazyl (DPPH) free radical scavenging activity. Int. J. Mol. Sci. 12, 3941–3949.
Donno, D., Cavanna, M., Beccaro, G.L., Mellano, M., Torello Marinoni, D., Cerutti, A.K., Bounous, G., 2013. Currants and strawberries as bioactive compound sources: determination of antioxidant profiles with HPLC-DAD/MS. J. Appl. Bot. Food Qual. 86, 1–10.
Encarnação, S., de Mello-Sampayo, C., Graça, N.A.G., Catarino, L., da Silva, I.B.M., Lima, B.S., Silva, O.M.D., 2016. Total phenolic content, antioxidant activity and pre-clinical safety evaluation of an *Anacardium occidentale* stem bark Portuguese hypoglycemic traditional herbal preparation. Ind. Crops Prod. 82, 171–178.
Ferrante, C., Orlando, G., Recinella, L., Leone, S., Chiavaroli, A., Di Nisio, C., Shohreh, R., Manippa, F., Ricciuti, A., Vacca, M., 2016. Central inhibitory effects on feeding induced by the adipo-myokine irisin. Eur. J. Pharmacol. 791, 389–394.
Ferreres, F., Gil-Izquierdo, Á., Andrade, P.B., Valentão, P., Tomás-Barberán, F.A., 2007. Characterization of C-glycosyl flavones O-glycosylated by liquid chromatography–tandem mass spectrometry. J. Chromatogr. A 1161, 214–223.
Fialkow, L., Wang, Y., Downey, G.P., 2007. Reactive oxygen and nitrogen species as signaling molecules regulating neutrophil function. Free Radic. Biol. Med. 42, 153–164.
Fu, Y., Zhou, X., Chen, S., Sun, Y., Shen, Y., Ye, X., 2015. Chemical composition and antioxidant activity of Chinese wild raspberry (*Rubus hirsutus* Thunb.). LWT Food Sci. Technol. 60, 1262–1268.
George, B.P., Abrahamse, H., Hemmaragala, N.M., 2017. Phenolics from *Rubus fairholmianus* induces cytotoxicity and apoptosis in human breast adenocarcinoma cells. Chem. Biol. Interact. 275, 178–188.
Gevrenova, R., Badjakov, I., Nikolova, M., Doichinova, I., 2013. Phenolic derivatives in raspberry (*Rubus* L.) germplasm collection in Bulgaria. Biochem. Syst. Ecol. 50, 419–427.
Goggins, M.G., Shah, S.A., Goh, J., Cherukuri, A., Weir, D.G., Kelleher, D., Mahmud, N., 2001. Increased urinary nitrite, a marker of nitric oxide, in active inflammatory bowel disease. Mediat. Inflamm. 10, 69–73.
Han, N., Gu, Y., Ye, C., Cao, Y., Liu, Z., Yin, J., 2012. Antithrombotic activity of fractions and components obtained from raspberry leaves (*Rubus chingii*). Food Chem. 132, 181–185.
Herbrechter, R., Ziemba, P.M., Hoffmann, K.M., Hatt, H., Werner, M., Gisselmann, G., 2015. Identification of Glycyrrhiza as the rikkunshito constituent with the highest antagonistic potential on heterologously expressed 5-HT3A receptors due to the action of flavonoids. Front. Pharmacol. 6, 130.
Hummer, K.E., 2010. Rubus pharmacology: antiquity to the present. Hortscience 45, 1587–1591.
Huot, B., Yao, J., Montgomery, B.L., He, S.Y., 2014. Growth–defense tradeoffs in plants: a balancing act to optimize fitness. Mol. Plant 7, 1267–1287.
Jung, S.W., Shin, M.H., Jung, J.H., Kim, N.D., Im, K.S., 2001. A triterpene glucosyl ester from the roots of *Rubus crataegifolius*. Arch. Pharm. Res. 24, 412–415.
Kannan, N., Guruvayoorappan, C., 2013. Protective effect of *Bauhinia tomentosa* on acetic acid induced ulcerative colitis by regulating antioxidant and inflammatory mediators. Int. Immunopharmacol. 16, 57–66.
Keser, S., Çelik, S., Turkoglu, S., Yilmaz, Ö., Turkoglu, I., 2015. Antioxidant properties of *Rubus discolor* L. extracts and protective effects of its flower extract against hydrogen peroxide-induced oxidative stress in wistar rats. Turkish J. Pharm. Sci. 12, 89–111.
Kim, C.R., Choi, S.J., Oh, S.S., Kwon, Y.K., Lee, N.Y., Park, G.G., Kim, Y.-J., Heo, H.J., Jun, W.J., Park, C.-S., 2013. *Rubus coreanus* Miquel inhibits acetylcholinesterase activity and prevents cognitive impairment in a mouse model of dementia. J. Med. Food 16, 785–792.
Kruidenier, L.a., Verspaget, H., 2002. Oxidative stress as a pathogenic factor in inflammatory bowel disease—radicals or ridiculous? Aliment. Pharmacol. Ther. 16, 1997–2015.
Lee, J., Dossett, M., Finn, C.E., 2012. Rubus fruit phenolic research: the good, the bad, and the confusing. Food Chem. 130, 785–796.
Li, Q., He, S., Chen, Y., Feng, F., Qu, W., Sun, H., 2018. Donepezil-based multi-functional cholinesterase inhibitors for treatment of Alzheimer's disease. Eur. J. Med. Chem. 158, 463–477.
Lobo, V., Patil, A., Phatak, A., Chandra, N., 2010. Free radicals, antioxidants and functional foods: impact on human health. Pharmacogn. Rev. 4, 118–126.
Locatelli, M., Ferrante, C., Carradori, S., Secci, D., Leporini, L., Chiavaroli, A., Leone, S., Recinella, L., Orlando, G., Martinotti, S., 2017. Optimization of aqueous extraction and biological activity of *Harpagophytum procumbens* root on ex vivo rat colon inflammatory model. Phytother Res. 31, 937–944.
Menghini, L., Ferrante, C., Leporini, L., Recinella, L., Chiavaroli, A., Leone, S., Pintore, G., Vacca, M., Orlando, G., Brunetti, L., 2016. An hydroalcoholic chamomile extract modulates inflammatory and immune response in HT29 cells and isolated rat colon. Phytother Res. 30, 1513–1518.
Menghini, L., Leporini, L., Vecchiotti, G., Locatelli, M., Carradori, S., Ferrante, C., Zengin, G., Recinella, L., Chiavaroli, A., Leone, S., 2018. *Crocus sativus* L. stigmas and by products: qualitative fingerprint, antioxidant potentials and enzyme inhibitory activities. Food Res. Int. 109, 91–98.
Mihara, M., Uchiyama, M., Fukuzawa, K., 1980. Thiobarbituric acid value on fresh homogenate of rat as a parameter of lipid peroxidation in aging, CCl4 intoxication, and vitamin E deficiency. Biochem. Med. 23, 302–311.
Mousavizadeh, K., Rahimian, R., Fakhfouri, G., Aslani, F., Ghafourifar, P., 2009. Anti-inflammatory effects of 5-HT3 receptor antagonist, tropisetron on experimental colitis in rats. Eur. J. Clin. Invest. 39, 375–383.
Nagarjun, S., Dhadde, S.B., Veerapur, V.P., Thippeswamy, B., Chandakavathe, B.N., 2017. Ameliorative effect of chromium-D-phenylalanine complex on indomethacin-induced inflammatory bowel disease in rats. Biomed. Pharmacother. 89, 1061–1066.
Ohikhena, F.U., Wintola, O.A., Afolayan, A.J., 2016. Toxicity assessment of different solvent extracts of the medicinal plant, *Phragmanthera capitata* (sprengel) balle on brine shrimp (*Artemia salina*). Int. J. Pharmacol. 12, 701–710.
Oliveira, B.D.Á., Rodrigues, A.C., Cardoso, B.M.I., Ramos, A.L.C.C., Bertoldi, M.C., Taylor, J.G., Cunha, L.R.d., Pinto, U.M., 2016. Antioxidant, antimicrobial and anti-quorum sensing activities of *Rubus rosaefolius* phenolic extract. Ind. Crops Prod. 84, 59–66.
Oszmiański, J., Wojdyło, A., Nowicka, P., Teleszko, M., Cebulak, T., Wolanin, M.J.M., 2015. Determination of phenolic compounds and antioxidant activity in leaves from wild *Rubus L.* species. Molecules 20, 4951–4966.
Papaioanou, M., Chronopoulou, E.G., Ciobotari, G., Efrose, R.C., Sfichi-Duke, L., Chatzikonstantinou, M., Pappa, E., Ganopoulos, I., Madesis, P., Nianiou-Obeidat, I., 2018. Cosmeceutical properties of two cultivars of red Raspberry grown under different conditions. Cosmetics 5, 20–38.
Raihan, S.Z., Chowdhury, A.A., Rabbani, G.H., Marni, F., Ali, M.S., Nahar, L., Sarker, S.D., 2009. Effect of aqueous extracts of black and green teas in arsenic-induced toxicity in rabbits. Phytother Res. 23, 1603–1608.
Regmi, S.C., Park, S.-Y., Ku, S.K., Kim, J.-A., 2014. Serotonin regulates innate immune responses of colon epithelial cells through Nox2-derived reactive oxygen species. Free Radic. Biol. Med. 69, 377–389.
Ryu, J., Kim, W.J., Im, J., Kim, S.H., Lee, K.-S., Jo, H.-J., Kim, E.-Y., Kang, S.-Y., Lee, J.-H., Ha, B.-K., 2018. Genotyping-by-sequencing based single nucleotide polymorphisms enabled Kompetitive Allele Specific PCR marker development in mutant Rubus genotypes. Electron. J. Biotechnol. 35, 57–62.
Saijo, F., Milsom, A.B., Bryan, N.S., Bauer, S.M., Vowinkel, T., Ivanovic, M., Andry, C., Granger, D.N., Rodriguez, J., Feelisch, M., 2010. On the dynamics of nitrite, nitrate and other biomarkers of nitric oxide production in inflammatory bowel disease. Nitric Oxide 22, 155–167.
Sandjo, L.P., Nascimento, M.V.d.S., da Silva, L.A., Munhoz, A.C., Pollo, L.A., Biavatti, M.W., Ngadjui, B.T., Opatz, T., Fröde, T., 2017. ESI-MS2 and anti-inflammatory studies of cyclopropanic triterpenes. UPLC-ESI-MS and MS2 search of related metabolites from *Donella ubanguiensis*. Phytochem. Anal. 28, 27–41.
Shin, J.S., Cho, E.J., Choi, H.E., Seo, J.H., An, H.J., Park, H.J., Cho, Y.W., Lee, K.T., 2014. Anti-inflammatory effect of a standardized triterpenoid-rich fraction isolated from *Rubus coreanus* on dextran sodium sulfate-induced acute colitis in mice and LPS-induced macrophages. J. Ethnopharmacol. 158, 291–300.
Soliman, N., Keshk, W., Rizk, F., Ibrahim, M., 2019. The possible ameliorative effect of simvastatin versus sulfasalazine on acetic acid induced ulcerative colitis in adult rats. Chem. Biol. Interact. 298, 57–65.
Spínola, V., Pinto, J., Llorent-Martínez, E.J., Tomás, H., Castilho, P.C., 2019. Evaluation of *Rubus grandifolius* L. (wild blackberries) activities targeting management of type-2 diabetes and obesity using in vitro models. Food Chem. Toxicol. 123, 443–452.
Süntar, I., Koca, U., Keleş, H., Akkol, E.K., 2011. Wound healing activity of *Rubus sanctus* Schreber (Rosaceae): preclinical study in animal models. J. Evid. Based Complementary Altern. Med. 2011, 1–6.
Uttara, B., Singh, A.V., Zamboni, P., Mahajan, R., 2009. Oxidative stress and neurodegenerative diseases: a review of upstream and downstream antioxidant therapeutic options. Curr. Neuropharmacol. 7, 65–74.
Uysal, S., Zengin, G., Locatelli, M., Bahadori, M.B., Mocan, A., Bellagamba, G., De Luca, E., Mollica, A., Aktumsek, A., 2017. Cytotoxic and enzyme inhibitory potential of two *Potentilla* species (*P. speciosa* L. and *P. reptans* Willd.) and their chemical composition. Front. Pharmacol. 8, 290.
Uysal, A., Ozer, O.Y., Zengin, G., Stefanucci, A., Mollica, A., Picot-Allain, C.M.N., Mahomoodally, M.F., 2019. Multifunctional approaches to provide potential

pharmacophores for the pharmacy shelf: *Heracleum sphondylium* L. subsp. *ternatum* (Velen.). Brummitt. Comput. Biol. Chem. 78, 64–73.
Veličković, I.Z., Grujić, S.M., Marin, P.D., 2016. Antioxidant properties of *Rubus discolor* leaf extracts. Matica Srpska J. Nat. Sci. 131, 189–196.
Venskutonis, P.R., Dvaranauskaite, A., Labokas, J., 2007. Radical scavenging activity and composition of raspberry (*Rubus idaeus*) leaves from different locations in Lithuania. Fitoterapia 78, 162–165.
Verma, R., Gangrade, T., Punasiya, R., Ghulaxe, C., 2014. Rubus fruticosus (blackberry) use as an herbal medicine. Pharmacogn. Rev. 8, 101–104.
Xu, Y., Li, L.-Z., Cong, Q., Wang, W., Qi, X.-L., Peng, Y., Song, S.-J., 2017. Bioactive lignans and flavones with in vitro antioxidant and neuroprotective properties from *Rubus idaeus* rhizome. J. Funct. Foods 32, 160–169.
Zengin, G., Aktumsek, A., Ceylan, R., Uysal, S., Mocan, A., Guler, G.O., Mahomoodally, M.F., Glamoclija, J., Ciric, A., Sokovic, M., 2017. Shedding light on the biological and chemical fingerprints of three *Achillea* species (*A. biebersteinii, A. millefolium* and *A. teretifolia*). Food Funct. 8, 1152–1165.
Zengin, G., Rodrigues, M.J., Abdallah, H.H., Custodio, L., Stefanucci, A., Aumeeruddy, M.Z., Mollica, A., Rengasamy, K.R.R., Mahomoodally, M.F., 2018. Combination of phenolic profiles, pharmacological properties and in silico studies to provide new insights on Silene salsuginea from Turkey. Comput. Biol. Chem. 77, 178–186.
Zheleva-Dimitrova, D., Gevrenova, R., Zaharieva, M.M., Najdenski, H., Ruseva, S., Lozanov, V., Balabanova, V., Yagi, S., Momekov, G., Mitev, V.J.P.A., 2017. HPLC-UV and LC–MS Analyses of acylquinic acids in *Geigeria alata* (DC) Oliv. & Hiern. and their contribution to antioxidant and antimicrobial capacity. Phytochem. Anal. 28, 176–184.
Zheleva-Dimitrova, D., Zengin, G., Balabanova, V., Voynikov, Y., Lozanov, V., Lazarova, I., Gevrenova, R., 2018. Chemical characterization with in vitro biological activities of *Gypsophila* species. J. Pharm. Biomed. Anal. 155, 56–69.